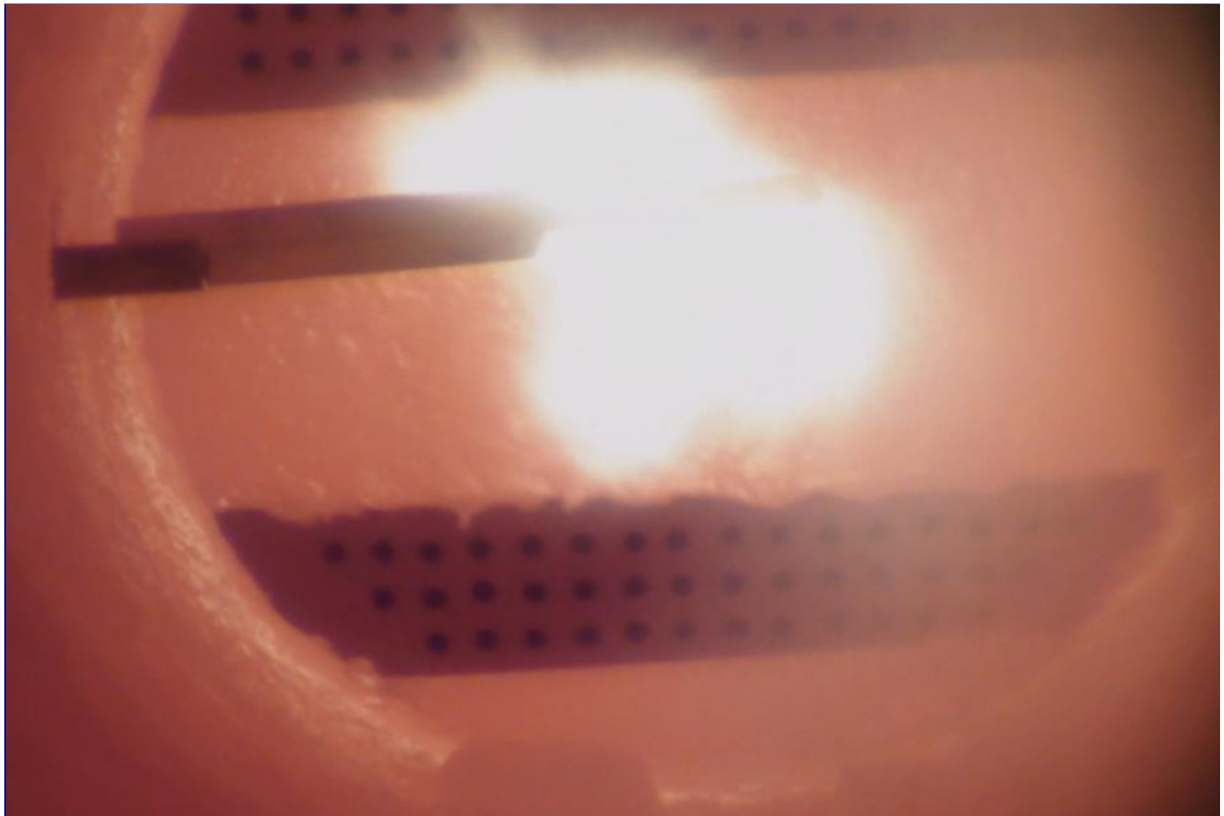


CHALMERS



Evaluation of the NO_x formation in a rotary kiln test facility

Master's Thesis within the Sustainable Energy Systems programme

JOHANNES HAUS

Department of Energy and Environment
Division of Energy Technology
CHALMERS UNIVERSITY OF TECHNOLOGY
Göteborg, Sweden 2014

MASTER'S THESIS

Evaluation of the NO_x formation in a rotary kiln test facility

Master's Thesis within the *Sustainable Energy Systems* programme

JOHANNES HAUS

SUPERVISOR:

Fredrik Normann

EXAMINER

Klas Andersson

Department of Energy and Environment

Division of Energy Technology

CHALMERS UNIVERSITY OF TECHNOLOGY

Göteborg, Sweden 2014

Evaluation of the NO_x formation in a rotary kiln test facility

Master's Thesis within the *Sustainable Energy Systems* programme
JOHANNES HAUS

© Johannes Haus, 2014

Department of Energy and Environment
Division of Energy Technology
Chalmers University of Technology
SE-412 96 Göteborg
Sweden
Telephone: + 46 (0)31-772 1000

Cover:

Picture taken from combustion video of oil inside the rotary kiln test facility

Chalmers Reproservice
Göteborg, Sweden 2014

Abstract

The rotary kiln process for iron ore pelletizing is one of the main methods to upgrade crude iron ore. The mining company LKAB runs four Grate-Kiln production sites in northern Sweden, where a grate and a rotary kiln are combined to thermally indurate the iron ore pellets. The high temperature needed for the process is provided by combustion of coal with a high amount of extremely preheated air, what creates an atmosphere inside the furnace of which the present theoretical understanding is low. So far, the high amount of excess air ($\lambda = 5-6$) made standard NO_x mitigation strategies in the rotary kiln unsuitable. Environmental issues and need for fuel flexibility has enticed LKAB to carry out experimental campaigns in a test facility to characterize the combustion process. The results of the experimental campaign of 2013 and previous campaigns are reviewed in the present work. The measurement results were evaluated through gas-phase chemistry modelling with a detailed chemical reaction scheme. The evaluation of the 2013 experimental campaign suggests measurement problems of the temperature and the combustion behaviour inside the test furnace. Gas and oil flames showed to combust almost instantaneously within the first centimetres after the burner. Biomass and coal combusted significantly slower, but also had the highest reaction intensity close to the burner inlet. Measured exhaust NO_x levels could not be achieved in the model with the measured temperature and modelling results proposed peak temperatures more than 500°C above the measured temperature inside the kiln for oil and gas combustion. For oil and gas it was found that thermal-NO_x is the major contributor to the NO_x formation inside the pilot scale kiln. The lower NO_x emissions for coal and biomass were explained by lower temperatures inside the kiln and the relation fuel-N and thermal-N. Modelling fuel bound nitrogen for the solid fuels showed that the NO_x is formed there in similar amounts via both the fuel-NO and thermal-NO formation route. By comparing the high NO_x levels of the experimental to the lower levels in the full scale plant, it was concluded that the NO_x formation differs between them, as in the experimental one significantly higher temperature prevail for all fuels. This showed that this facility does not resemble the actual kiln adequately.

Key words: NO_x formation, Iron ore pelletizing, high temperature combustion, gas-phase chemistry combustion modelling, gas, oil and coal combustion

Contents

ABSTRACT	I
CONTENTS	II
PREFACE	IV
LIST OF FIGURES	V
LIST OF TABLES	VI
ABBREVIATIONS AND SYMBOLS	VII
1. INTRODUCTION	1
1.1. Background	1
1.2. Aim and scope	2
2. IRON ORE PROCESSING	3
2.1. Grate-Kiln process	4
3. THEORY	7
3.1. NO _x formation	7
3.2. NO _x Modelling	8
4. METHODOLOGY	11
4.1. Previous experimental campaigns	11
4.2. General experimental setup	11
4.3. Measurement technique	12
4.4. Experimental campaign 2013	12
4.5. CHEMKIN simulations	15
5. MODELLING NO _x FORMATION	23
5.1. Gas-phase chemistry analysis of experiments	23
5.2. Summary of the gas-phase chemistry modelling	28
5.3. Sensitivity analysis for gas-phase chemistry	29
5.4. Impact of fuel nitrogen on NO _x formation	31

5.5.	Sensitivity analysis of the fuel-NO contribution	34
5.6.	Summary of the modelling work on fuel nitrogen	37
6.	CONCLUSIONS	39
7.	PROPOSALS FOR FUTURE CAMPAIGNS	39
7.1.	Improving the measurement quality	41
7.2.	Comparing NO _x formation in full scale and pilot scale	41
7.3.	Future modelling of the NO _x formation	42
8.	BIBLIOGRAPHY	43

Preface

This is the public version of the work on NO_x formation in a rotary kiln test facility. In this study modelling work of the NO_x formation in the facility is carried out. The modelling is based on confidential experimental data, which is not presented in this work. The thesis is part of a research collaboration of Chalmers University of Technology and the iron ore company LKAB in the field of emission formation. The experimental campaign was conducted in autumn 2013 at LKABs test facility in Luleå, Sweden. The project is carried out at the Department of Energy and Environment, Energy Technology, Chalmers University of Technology, Sweden.

The modelling part of the thesis was written with guidance of Assistant Professor Fredrik Normann as a supervisor and main source of information about the NO_x formation and its modelling and Associate Professor Klas Andersson as Examiner and extended knowledge about combustion phenomena. Daniel Bäckstrom, a PhD student at Chalmers, was assisting with information about the experimental campaign and his observations of radiative heat transfer inside the experimental kiln. The experiments were carried out by staff of the experimental facility of Swerea MEFOS under supervision of Christian Fredriksson.

Finally, I would like to thank these people for their steady support during the thesis and the availability and willingness to discuss problems occurring in the course of the work.

Göteborg, June 2014

Johannes Haus

List of figures

Figure 2-1: Iron ore processing pathways	3
Figure 2-2: Functioning of the Grate-Kiln process	5
Figure 3-1: Pathways for fuel-N	7
Figure 3-2: Plug flow reactor model	9
Figure 4-1: Outside side view of the ECF.	11
Figure 4-2: Sampling with a measurement probe inside the furnace.	12
Figure 4-3: Experimental data at different positions	15
Figure 4-4: Mixing profile used for modelling	16
Figure 4-5: Measured temperature profiles used for the simulations.....	16
Figure 4-6: Schematic view of the furnace with the inlet streams and the main phenomena	17
Figure 4-7: Idealized temperature profile shape used for fitting and sensitivity analysis.	18
Figure 4-8: Changed mixing behavior for the sensitivity analysis.	19
Figure 4-9: Accounting for fuel and oxidizer mixing behavior for solid fuels.	20
Figure 4-10: Temperature profiles used for the sensitivity analysis of solid fuels.	20
Figure 5-1: Adiabatic flame temperature for the furnace mixing conditions.....	24
Figure 5-2: Concentrations of CO, CO ₂ and O ₂ in different burner distances	24
Figure 5-3: Temperature profiles with different heat loss distributions.....	26
Figure 5-4: Results of fitting the peak temperature and peak location to the measured NO _x levels. ...	27
Figure 5-5: Comparison of NO _x generation of the simulation results with the measurements..	27
Figure 5-6: Thermal and Non-Thermal-NO formation rates for 2095°C peak at 25 cm..	28
Figure 5-7: NO _x exhaust concentration for different temperature peak locations	29
Figure 5-8: NO _x generated considering different mixing patterns	30
Figure 5-9: Modelled species for solid particle combustion.	32
Figure 5-10: Modelling result for a coal temperature profile.	33
Figure 5-11: Modelling result for a co-firing temperature profile at 1800°C	34
Figure 5-12: Influence of fuel-N on total NO _x formation. Fuel-N modelled as HCN compound in fuel.	35
Figure 5-13: Influence of different temperature levels on total NO _x formation.	35
Figure 5-14: Influence of difference fuel release profiles on the total NO _x formation.	36
Figure 5-15: Influence of the oxidizer mixing on the total NO _x formation.....	36

List of tables

Table 4-1: The fuels used in the experimental campaign.	13
Table 4-2: General inlet conditions for all fuels.	14
Table 4-3: Sensitivity analysis parameters of the gas-phase model for NO _x formation.....	18
Table 4-4: Sensitivity analysis parameters for the fuel-N release investigation.....	21
Table 4-5: Assumptions to simplify the modelling.	21
Table 5-1: Heat losses from the furnace for oil combustion.....	25
Table 5-2: Heat losses from the furnace for natural gas combustion.....	25
Table 5-3: Effects of adding fuel-N	31
Table 5-4: Comparison of the different furnaces according to their NO _x formation.....	37

Abbreviations and Symbols

Abbreviations

LKAB	Luossavaara-Kiirunavaara Aktiebolag
SCR and SNCR	Selective (Non) Catalytic Reduction
KK2	Kiruna Kulsinterverket 2 (Full scale pelletizing plant)
ECF	Experimental Combustion Furnace (Pilot scale model of KK2)
PFR	Plug Flow Reactor
CSR	Continuously Stirred reactor
NG	Natural Gas
EO5	Firing Oil 5 (“Eldningsolja 5”)
HHV	Higher Heating Value [MJ/kg]

Greek Symbols

λ	Air-to-Fuel ratio
ΔH	Enthalpy difference

Latin Symbols

CO_2	Carbon Dioxide
CO	Carbon Monoxide
O_2	Oxygen
NO_x	General term for Nitrogen Oxides
NO	Nitric Oxide or Nitrogen Monoxide
N_2O	Nitrous oxide or laughing gas
SO_2	Sulphur Dioxide
N_2	Nitrogen Oxide
HCN	Hydrogen Cyanide
H_2O	Dihydrogen Oxide, Water
NH_3	Ammonia
CH, O, N	General term for hydrocarbon, oxygen and nitrogen radicals
C_{XY}	Concentration of different species

1. Introduction

1.1. Background

The demand for iron ore has become an indicator for the economic development of countries around the globe. Especially the developing countries' demand for iron ore continues unabated and the global steel production hits new records annually [1]. Thus, it is foreseen that the iron ore mining and processing in Kiruna, northern Sweden, will be economically feasible for the coming decades.

The state owned company Luossavaara-Kiirunavaara Aktiebolag (LKAB) is processing the iron ore after extraction on-site in the Kiruna area to iron ore pellets. The thermal part of the process, where iron ore is sintered to pellets, requires very high temperatures and has to be carried out in special kilns. One of the equipment options is a combination of a straight grate and a rotary kiln, where the pellets are heated, dried and oxidized by extremely preheated air and the combustion of coal.

The emission of carbon dioxide (CO_2) from the use of coal in the iron ore processing, because of its contribution to global warming, is of current concern for the iron-producing industry. This is why LKAB and Chalmers University of Technology have an on-going research project that aims to increase the fuel flexibility in the iron production to decrease fuel costs and emissions of CO_2 . The choice of fuel has a major impact on the combustion situation and, with it, the formation of other important pollutants, like nitrogen oxides (NO_x).

The emission of NO_x is a source of acid rain and smog [2], which is the reason why the formation of nitrogen oxides is a focus point during the research in LKAB's rotary kilns. In this kind of large scale facility, both primary measures, like adjustments in the combustion process and burner configuration, and secondary measures, like SNCRs and SCR facilities, can be applied to decrease the NO_x exhaust to desired levels. Primary measures have usually an economical advantage over secondary ones as they do not need extensive new equipment and/or have no additional consumption of substances.

The burner configuration in a rotary kiln for iron ore production is relatively unique, with extreme air excess and air preheating, and the fundamental knowledge about its combustion behaviour is therefore limited. As NO_x formation depends heavily on the combustion situation, this fundamental knowledge about the reaction conditions is needed to optimize the operation of the LKAB rotary kiln for low NO_x levels, without compromising the conditions required for pellet production.

Within the next years, the combustion and heat transfer conditions related to choice of fuel in rotary kilns is investigated during the research cooperation of LKAB and Chalmers University of Technology; processes which will be influenced by the combustion conditions and the burner arrangement. The iron making process itself may also influence the emission formation and the radiative heat transfer conditions by means of for example heat release in the production process as mentioned above.

For a better understanding of the combustion inside kilns experiments are performed and evaluated and models of the operation are derived. During fall 2013 a first measurement campaign dedicated to fuel flexibility was performed in LKABs 400 kW_{th} experimental test facility that resembles the conditions in the full scale rotary kiln, called KK2. The campaign generated experimental data on NO_x formation and flame radiation from different fuels, including coal, gas and biomass. Together

with field data from LKAB's production facilities from previous measurement campaigns during the years 2008-2012 these measurements are the basis of the evaluation of combustion, emission formation and heat transfer issues of interest in the rotary kiln.

1.2. Aim and scope

The purpose of this work is to characterize the NO_x formation in rotary kilns by evaluating the experimental data from the measurement campaign in 2013 in the rotary kiln test facility, the Experimental Combustion Furnace ECF.

Furthermore modelling is carried out to give a deeper insight in the combustion chemistry of the fuels investigated. The aim is to map the NO_x formation during the combustion with different fuels and temperature conditions in the rotary kiln. The results from the ECF are applied to discuss also the emission formation in the full scale unit.

With the help of the experimental evaluation and the modelling work, focus areas and improvements should be proposed for the upcoming experimental campaign during 2014 as well as for the continued modelling work of the process.

2. Iron ore processing

There are several alternatives and routes to process and use mined iron ore and which route is chosen depends on a variety of factors, for example the needed quality, the grade of the mined iron ore or its later purpose in the steel industry. As indicated in Figure 2-1, three main refined products can be found in the iron ore industry, the rather unprocessed lump ore, the iron ore sinter and the iron ore pellets.

Despite its long history, the iron ore pelletizing did not become commercial before the Second World War. The development of the pelletizing process was mainly driven by the desire of using lower grade iron ore resources and the pelletizing enriches the iron content to the requirements in blast furnaces [3].

The iron ore that is mined by LKAB in the world's two largest underground iron ore mines in Kiruna and Malmberget [4] is mostly processed to pellets, despite the fact that the iron ore from the iron ore body in Kiruna has unlike most other resources in the world high iron ore content [5]. The reason for still using this more intensive processing route is that it is much easier to transport the iron after the pelletizing process compared to shipping the lump iron directly. Furthermore iron ore pellets have proven to be fortunate in the steelmaking process due to increased permeability for air compared to normal sinter. The possible pathways of iron ore processing are shown in Figure 2-1.

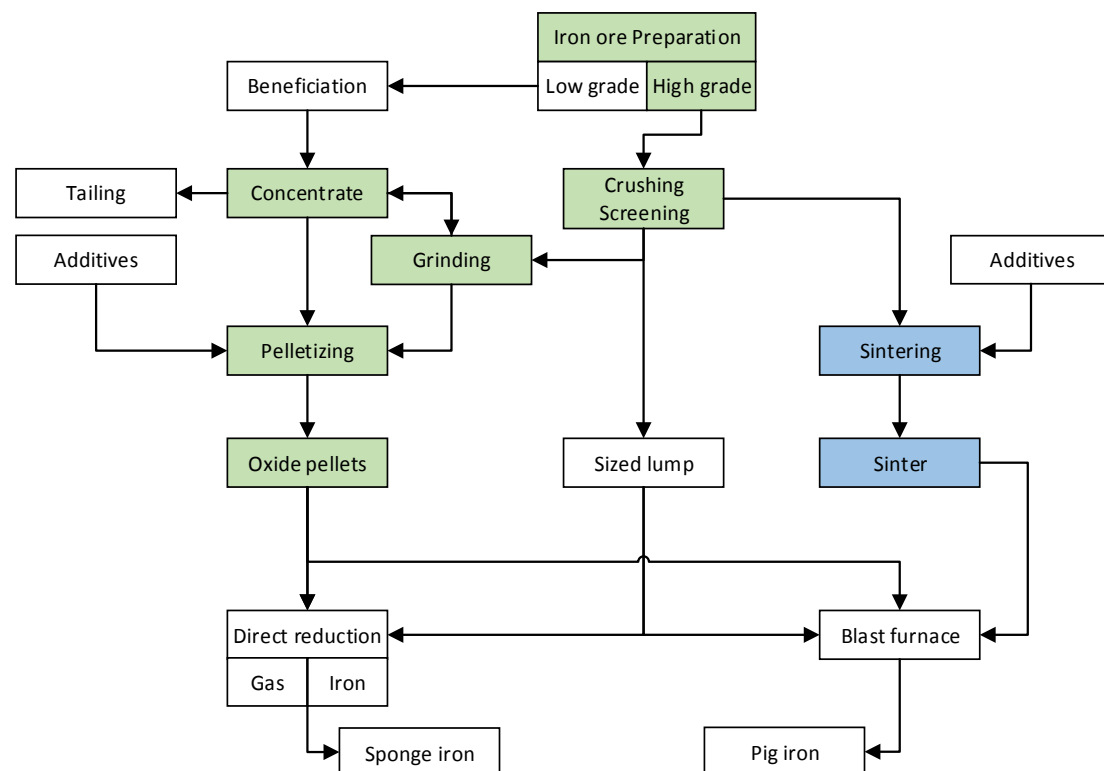


Figure 2-1: Iron ore processing pathways [3]. Highlighted green are the processes taking place at LKAB sites in Kiruna described in this work. Also sintering of the fines takes place in Kiruna, but on a much smaller scale (blue).

Presented in the Figure 2-1, the iron ore from Kiruna is crushed and sorted directly after mining. Then the iron ore is concentrated and phosphorus is removed before fed into the pelletizing drums. Into the drums additives, like binders and substances for

the later processing, are added. In this process the so called green pellets are formed. The last step of processing is the thermal treatment of the green pellets, where the green pellets are fed towards a combination of a straight grate and rotary kiln sintering unit, together called the Grate-Kiln thermal process. In this process at first the ore is preheated and parts of it oxidized in the travelling grate and then moving further to the rotary kiln where the different layers of pellets are mixed and nearly completely oxidized at very high temperatures. This work focused on the combustion inside the Grate-Kiln processing step, which is further described below.

As regards the completeness, it has to be mentioned that small parts of the iron ore mined in Malmberget is processed to fines shown by the blue boxes in Figure 2-1. The other iron ore from Malmberget is also transformed into pellets but in a single straight grate process without a rotary kiln. The processed iron pellets and fines are transported to the harbours in Narvik, Norway and Lulea, Sweden, where it is shipped to LKAB's customers around the world [6].

2.1. Grate-Kiln process

The Grate-Kiln process is illustrated in Figure 2-2. The green pellets enter the drying stage and pass through the processes of drying and dehydration on the travelling grate. The heat is added by both updraft and downdraft air. The heaters are arranged to facilitate the dehydration by dispatching the evaporated water and minimize thermal exposure to the travelling grate. The oxidation starts before the rotary kiln, but is distributed unevenly within the pellet layer. The upper pellets are oxidized to a higher extend than the pellets lying closer to the grate.

The green pellets have to be thermally processed to withstand the forces that will act on them during transportation. The resilience of the pellets is a key design factor for both the green and the final pellets, i.e. the height of pellets bed entering the travelling grate is limited so that the weight of the upper layers does not crush the pellets below. But too strong green pellets are disadvantageous during oxidization and therefore the green pellet quality is steadily measured.

The uneven distribution of oxidization leads to the need of mixing the pellet layers to provide a homogenous quality of the pellets. This mixing can be achieved in the rotating kiln. Inside the kiln the pellets are heated up to the necessary 1250°C to 1300°C for oxidization. Fuel is combusted via an annular burner and with extremely preheated air of 1150°C that is inserted above and below the burner to reach the required temperatures in the pellet bed [7]. To provide more than 1250°C in the bed, it can be assumed that the combustion zone reaches a significantly higher temperature.

The preheated air stems from cooling demand of the finished pellets. It is fed completely back into the system and corresponds to around six times the air amount that would be actually needed for complete combustion of the fuel. This environment of extreme oxygen abundance is needed to convert the pellets during their oxidation processes. The oxidation of the pellets itself provides around 60% of the total energy demand.

Exiting the kiln, the pellets just fall down into the circular cooler where they are exposed to the cooling air, but the oxidation continues even in the cooler. After enormous amounts of air have cooled them down sufficiently to around 200°C, they can be discharged safely [8]. The cooling air is fed as combustion air to the burner but also to the preheating of the pellets.

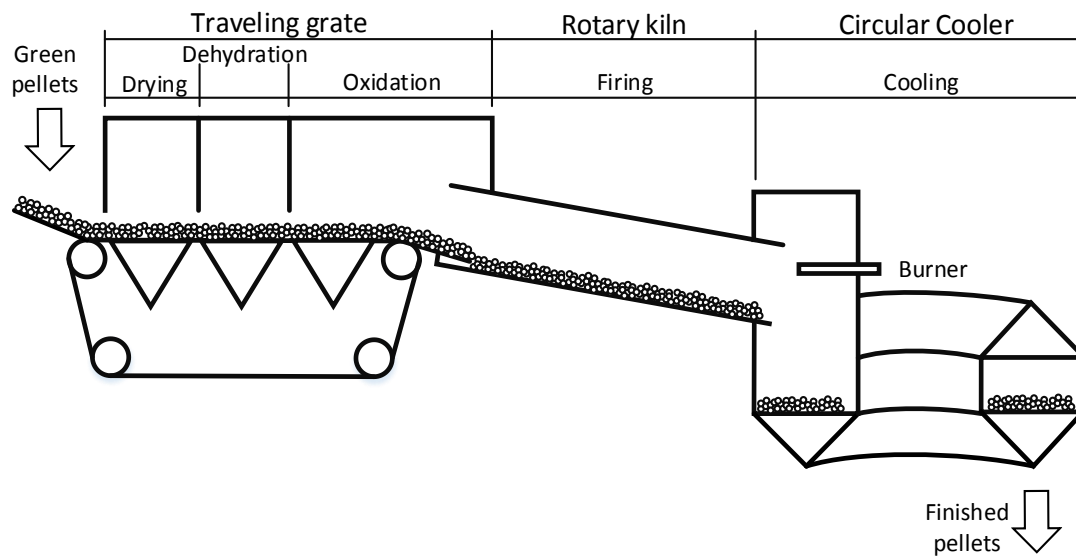


Figure 2-2: Functioning of the Grate-Kiln process from Meyer [3]. The green pellets run through the three different parts of the Grate-Kiln combination and leave as finished pellets.

3. Theory

This work mainly focuses on the evaluation of the NO_x formation inside the Experimental Combustion Furnace. NO_x can be traced mainly to three different formation mechanisms that will be described within this chapter. Afterwards the background of the NO_x modelling with a detailed chemical reaction scheme is explained.

3.1. NO_x formation

During the combustion process pollutants like sulphur dioxide SO_2 and nitrogen oxides, like NO and N_2O may form. The formation of these pollutants is undebated a cause for smog and ozone in cities and furthermore, nitrogen oxides can be a reason for acid rain [2].

The formation of nitrogen oxides may be divided into three main mechanisms. The first one is the release of nitrogen from the fuel itself, thus called fuel-N. The second mechanism, thermal- NO formation, as the name is implying is triggered by very high temperatures that cause nitrogen in the air to react. The last mechanism often described is the prompt- NO , which includes the formation of NO_x from the nitrogen in the air by the attack of hydrocarbon radicals. Warnatz et al. describe also a fourth mechanism in lean combustion conditions similar to the thermal nitrogen oxide formation, the N_2O mechanism [2]. There additionally other molecules are present why it is classified as a so called third body reaction.

FUEL-NO

For the generation of NO from fuel, there must be nitrogen present in the fuel. Therefore this aspect can be disregarded for the fuel oil and gas and is mainly important for the NO_x formation during solid fuel combustion.

Fuel-N is released during the devolatilization mostly in the form of NH_3 and HCN [9] that will react further to NO or N_2 depending on the combustion situation. The fuel-N released during devolatilization is called volatile-N. The nitrogen remaining in the particles in the coal is called char-N and can also react towards NO_x . A simplified pathway for fuel- NO is thereby shown in Figure 3-1. Whether the intermediate species react further to NO or N_2 is thereby dependent on different parameters, like oxygen presence and the temperature [10].

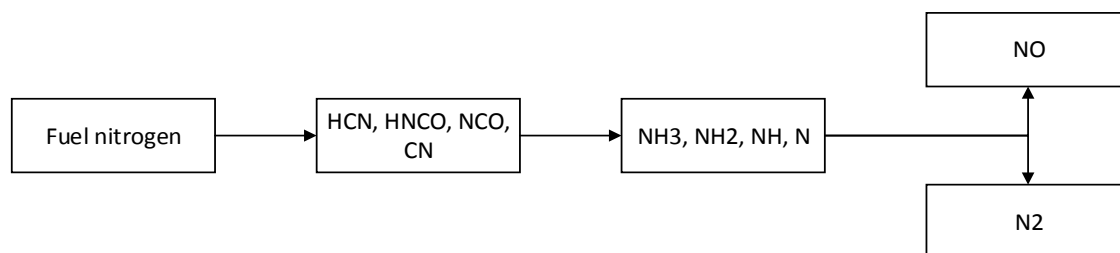


Figure 3-1: Pathways for fuel-N from Gardiner [11]. The final conversion to N_2 or NO is dependent on the combustion environment inside the furnace.

THERMAL-NO

Reviewing different literature about thermal-NO formation, it is steadily referred to the extended Zeldovich mechanism from 1946 [12]. As stated there, three main reactions are responsible for the formation of NO_x emissions. The reactions show the importance of oxygen, which has to be present to form NO_x emissions.



The reactions can occur in both directions and are mainly dependent on the concentrations of O₂ and the temperature. In the literature it is mentioned mostly that below 1700-1800 K this formation mechanism is insignificant. Hence, strategies to avoid thermal-NO focus mainly to reduce the O₂ concentration and diminish temperature peaks over 1700K [11].

PROMPT-NO

The last of the three most important NO_x formation pathways was first discovered by Fenimore [13], who tried to find an explanation of the formation of NO_x which could not be explained by the thermal-NO_x mechanism. He found out that NO_x is formed early during combustion when the necessary temperatures for thermal-NO are not met. The reason for this formation is the attack of hydrocarbon radicals on nitrogen of the combustion air. The main reaction for prompt-NO formation is given in Gardiner [11] as:



The same intermediate substance like in fuel-NO, the hydrogen cyanide, is formed as well as a nitrogen radical, that can both react further to NO as indicated in Figure 3-1.

3.2. NO_x Modelling

Reaction mechanism

The main reactions of NO_x formation were described, but it has to be noticed, that the global combustion and formation mechanisms take place via a vast amount of chemical reactions and intermediate products. This is the reason why detailed chemical reaction schemes are developed in various research groups that cover the NO_x formation in more detail than the global reactions from the chapter before.

The set of equations used in this work was latest revised by Mendiara and Glarborg [14] and goes back to the work of Miller in 1981 et al. with the title "A Chemical Kinetic Model for the Selective Reduction of Ammonia" [15]. The earlier mechanism was extended and validated in different environments and consists now of over 700 chemical reactions. To mention some research work that was done to establish this set of equations Skreiberg et al. [16], can be named, who examined the reaction path of ammonia or Dagaut et al. [17], who checked the hydrogen cyanide chemistry for solid fuel combustion. A more detailed description and evolution for the used mechanism can be found in various theses within the department [18].

Reactor model

The set of equations is then implemented into a reactor model that suits best to the conditions in the furnace. Two simplistic reactor models are commonly used in the

field of combustion engineering, the 0-dimensional Continuously Stirred Reactor (CSR) and the 1-dimensional Plug Flow Reactor (PFR). The CSR model is not applicable here, as it approximates the chemical reactions over a control volume at a steady temperature, whereas a detailed analysis of the chemistry at different temperatures inside the reactor is the main aim of this work. This is why a PFR model is applied that can “follow the progress of combustion in a system” [19]. In the PFR shown in Figure 3-2, the chemical reactions are calculated at different distances x from the reactor inlet.

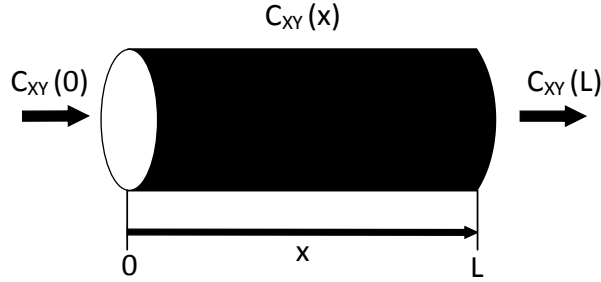


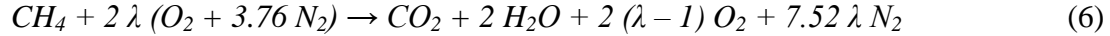
Figure 3-2: Plug flow reactor model [19].

Combustion modelling

The focus in this work is the formation of NO_x in the furnace, so the combustion itself is modelled with methane as fuel. The simplistic stoichiometric reaction therefore is:



Taking all species, that is the nitrogen and excess oxygen in the combustion air, into account that will be present during combustion, the overall reaction is:



It was described that enormous amounts of air enters the Grate-Kiln because of the recuperation of the heat in the cooler. With that air a high value of lambda is reached. Looking at reaction (6) it becomes clear that with the high values of lambda, the molar amount of fuel becomes small compared to nitrogen and oxygen and in this way the nitrogen chemistry becomes predominant.

4. Methodology

This work is divided into two parts. The first part is an evaluation of an experimental campaign denoted towards NO_x formation, but is not included in this paper. This part also includes a review of key findings from earlier experimental campaigns. The experimental setup is explained within the methodology chapter. This evaluation and its results will be the framework for the second part, the modelling work, which tries to explain in detail the NO_x formation and its underlying chemistry inside the ECF.

4.1. Previous experimental campaigns

Before the 2013 measurement campaign, other measurement campaigns solely denoted to NO_x reduction techniques were carried out in the time 2007-2012. The experimental campaigns were conducted in different combustion furnaces, on lab scale, in the pilot scale furnace ECF as well as the full scale rotary kiln KK2. The main findings of these campaigns are included to support the evaluation of the recent campaign.

4.2. General experimental setup

To investigate combustion and reaction behaviour during Grate-Kiln combustion in the pelletizing plant, a downscaled test unit resembling the kiln was deployed in the year 2007. This experimental furnace is called Experimental Combustion Furnace (ECF) and is placed in Luleå, Sweden. The furnace has a total length of around 12 meters and 0.8 m inner diameter. The main combustion air is fed above and below the burner as showed in Figure 4-1. The fuel is inserted with a central mounted burner.

In difference to the real KK2, the ECF is not rotating to facilitate the measurements that can be carried out at different ports along side of the reactor. Measurement tools, like temperature probes and a gas composition analyser can be inserted directly into the combustion. It is thus possible to create a radial profile inside the furnace of the gas composition and temperature.

The inlet conditions (fuel, air amount and temperature) were measured as well as the outlet condition and composition of the gases leaving the furnace after 12 m. To create a profile from the temperature and the species, data points along the furnace cross section were recorded.

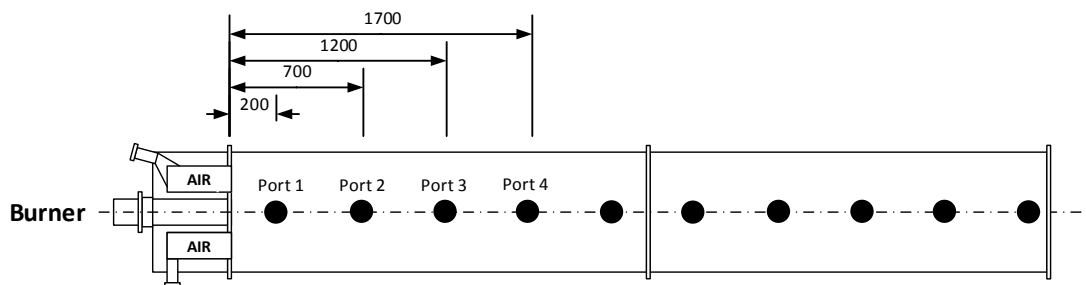


Figure 4-1: Outside side view of the ECF. The measurement ports and their distance to the centrally mounted burner are indicated. Below and above the burner, the inlets for the secondary air are sketched.

4.3. Measurement technique

For the measurements at the ports shown in Figure 4-1, a measurement probe presented in Figure 4-2 was inserted into the ports. Starting at 0 cm from the wall the probe moved towards the middle at 40 cm and the last data was taken at the opposite wall at 80 cm. The relevant species CO, CO₂, O₂, NO_x and SO₂ plus the temperatures were measured inside the furnace and at the furnace outlet, to create a radial profile inside the furnace and also get the outlet condition of the values. These measurements are the basis for an interpretation of combustion chemistry during the campaign.

A crucial factor in conduction temperature measurements with the suction probe is thereby the gas inlet velocity. Heitor and Moreira describe effects that can arise when suction pyrometers are not used properly and the probe inlet velocity is too low [20]. In their work, for a real flame temperature of 1000°C a 230°C lower temperature was measured due a faulty inlet velocity.

Measurements of the radiative heat transfer, which took place at the same time and is not part of this thesis, showed that the radiation intensity points at temperature peaks above 1800°C for the solid as well as the liquid and gaseous fuels.

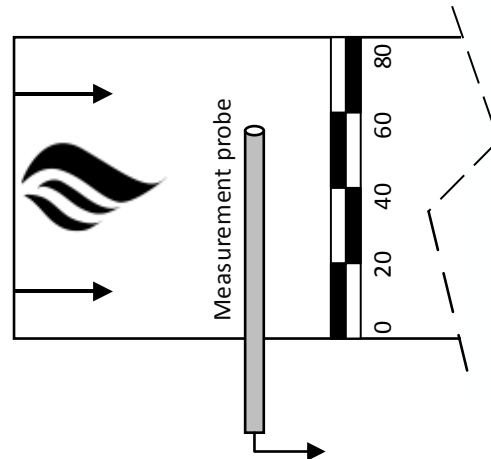


Figure 4-2: Sampling with a measurement probe inside the furnace.

4.4. Experimental campaign 2013

The 2013 campaign was dedicated towards different research needs with respect to fuel flexibility. Two aspects that were examined during the campaign and are not part of this thesis are the heat radiation of different fuels inside the combustion furnace and the examination of slag built-up inside the ECF. The main topic of this thesis is dedicated to the measurements of the formed nitrogen oxides during the combustion inside the furnace. The basic experimental order was the following:

- a) A fuel was introduced to the furnace and fired for about 6 hours to reach a steady combustion state.
- b) Then the composition and temperature of the gases and inside the furnace was measured at the different ports.
- c) After that, the radiative heat transfer was measured inside the furnace at different ports.
- d) The formation of slag was examined at last.
- e) The fuel was changed and process a-d) were started again.

For the coal measurements, all the measurements were carried out at port 1, 2 and 4 as presented in Figure 4-1. For the natural gas and oil combustion, only port 2 and 4 were used. Furthermore at port 1 only positions inside and close to the flame were measured.

Concluding, in the various research projects the same fuels and fuel blends were examined for the different research purposes. A complete list of the examined fuels is given in Table 4-1, where also the different burners used in the experiments are indicated. During the coal firing and the first biomass co-firing, with the letters C)-E) in the Table, the reference burner was used, which injected a pure stream of coal or a premix of the fuels. For the other co-firings F)-K), a burner was used that injected the fuels separately, originally called “kombibrännare” or combined burner. All the solid fuels were milled before combustion. The evolving biomass particles were much coarser than the milled coal.

Table 4-1: The fuels used in the experimental campaign are shown in chronological order of the experiments. The percentage of the composition represents the part of the fuel effect in kW.

Type		Name	Composition (fuel effect)	Burner
A	Oil	Eldningsolja 5 - Heavy fuel oil	100% Oil	Oil burner
B	Gas	Natural Gas	100% NG	Gas burner
C	Coal	Coal 1	100% Coal	Reference axial burner
D	Coal	Coal 2	100% Coal	Reference axial burner
E	Coal-Biomass-Co-Firing	Coal 1 and Biomass 1	70% Coal/30% Biomass	Reference axial burner
F	Coal-Biomass-Co-Firing	Coal 1 and Biomass 1	90% Coal/10% Biomass	Turbojet Kombiburner
G	Coal-Biomass-Co-Firing	Coal 1 and Biomass 1	70% Coal/30% Biomass	Turbojet Kombiburner
H	Coal-Biomass-Co-Firing	Coal 1 and Biomass 2	90% Coal/10% Biomass	Turbojet Kombiburner
I	Coal-Biomass-Co-Firing	Coal 1 and Biomass 2	70% Coal/30% Biomass	Turbojet Kombiburner
J	Coal-Biomass-Co-Firing	Coal 1 and Biomass 3	90% Coal/10% Biomass	Turbojet Kombiburner
K	Coal-Biomass-Co-Firing	Coal 1 and Biomass 3	70% Coal/30% Biomass	Turbojet Kombiburner

Inlet conditions

The inlet conditions of the experiments are presented in Table 4-1. They were extracted from the data sheets and are generally valid for all the fuels described. All the fuels were injected to amount for a fuel input of 400 kW and the same amount of combustion air was always inserted.

Table 4-2: General inlet conditions for all fuels.

Fuel input	400 kW
Temperature fuel	25°C (Oil: 90°C)
Combustion air above	1180 m ³ n/h
Combustion air below	1030 m ³ n/h
Temperature combustion air	1070 - 1100°C
Air to fuel ratio λ	5-6

4.5. CHEMKIN simulations

Modelling of the gas-phase NO_x formation inside the furnace was used to interpret the experiments and analyse the chemical reactions taking place as well as the overall combustion situation. The experimental data from the ECF was utilized as input data for the modelling work. The furnace was modelled as a plug flow reactor (PFR) shown schematically in Figure 4-3. The combustion and nitrogen chemistry was described by the detailed chemical reaction scheme proposed by Mendiara and Glarborg [14].

With the help of a simplified mixing and temperature data, the detailed reaction scheme calculates the underlying chemical reactions inside the ECF. The furnace demonstrated in Figure 4-3 could be interpreted as a reacting zone that is extending from a small area where only parts of the injected air is mixed with the fuel and later the combustion gases, towards the complete flow towards the outlet. The numbers indicate the measurements, which were used as input data. This approach has been previously used by for example Normann [18].

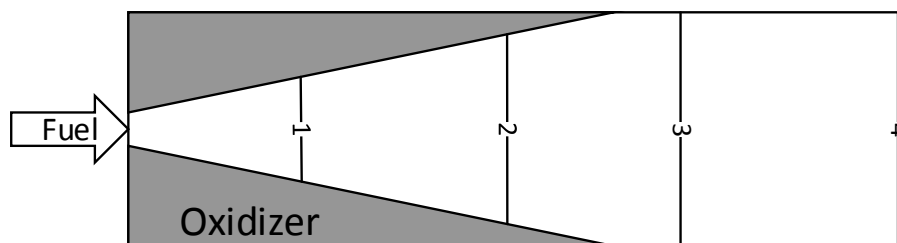


Figure 4-3: Experimental data at different positions 1, 2, 3 and 4 to be used for developing a mixing profile of fuel and oxidizer. The white area is modelled whereas the oxidizer enters the modelled zone during the course of the furnace.

Mixing conditions for the simulations

The idea of using a mixing profile is to implement effects of mixing without knowing the detailed mixing behaviour and fluid flow, what would require comprehensive analysis of the flow with CFD tools. From the experimental results, a main combustion zone where the combustion species CO , O_2 , CO_2 and NO_x are present in higher concentrations. Also a higher temperature than in the outer zone is found there. Hence, the main combustion zone and the measured species O_2 , CO_2 and NO_x inside are basis of the development of the mixing profile. For the modelling of natural gas and oil combustion, the mixing profile shown in Figure 4-4 was used. This profile was derived to match the measured species from the experimental data. Delaying effects during solid fuel combustion and with it the fuel-N release needed different fuel and oxidizer mixing profiles described in the section further below and in Figure 4-9.

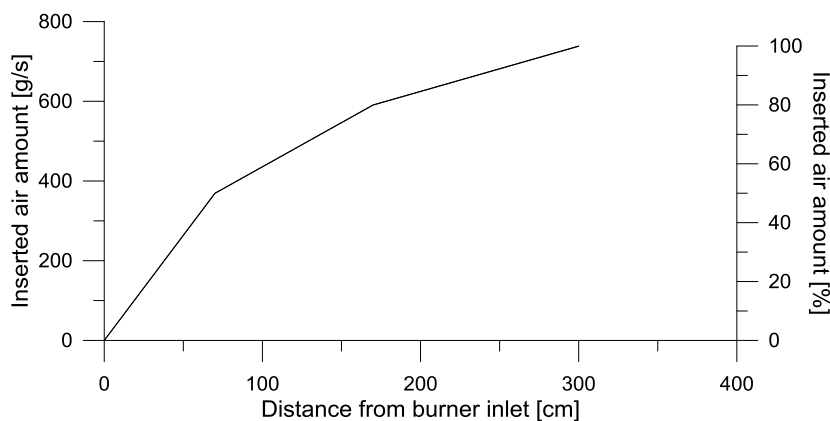


Figure 4-4: Mixing profile used for modelling based on experimental species concentrations during oil and gas combustion. The combustion air amount totals 740 g/s.

Temperature data for the simulations

After having developed the mixing behaviour inside the reactor, temperature information has to be fed into the model to receive accurate simulation results of the NO_x formation inside the furnace. Four approaches to determine the temperature profile of the ECF has been used throughout the investigation.

A) Measured temperature profiles

The temperature profiles measured during the experiments were directly used in the chemical reaction modelling. The measured profiles are shown in Figure 4-5. Also the coal and co-firing profiles were examined to clarify whether the reactions follow a simplistic gas-phase modelling approach.

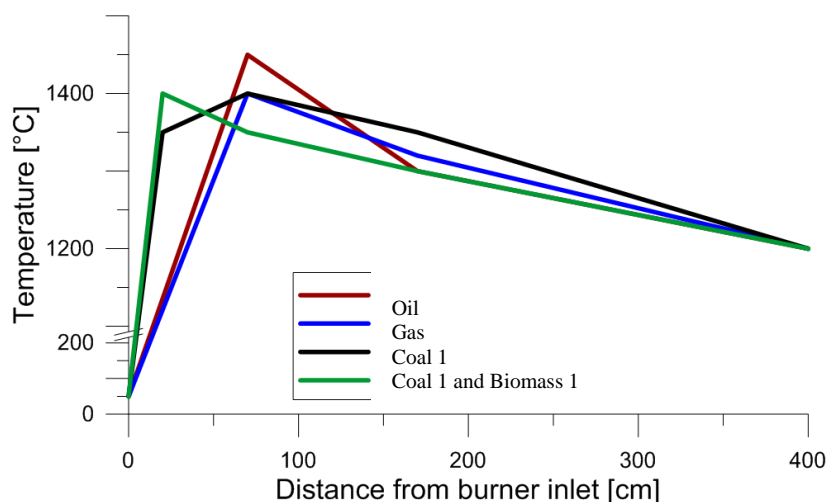


Figure 4-5: Measured temperature profiles used for the simulations and validation of the measurement results.

B) Adiabatic combustion simulations

An adiabatic combustion temperature profile was used as a theoretical maximum and to create a picture of a possible shape of the temperature distribution inside the furnace. For this simulation, only the inlet temperatures and a mixing behavior of fuel and oxidizer have to be inserted and from there the resulting temperature conditions can be calculated.

C) Energy balances

Another temperature profile was determined combining the adiabatic results and energy observations. This approach included an energy balance over the furnace to see how much energy is lost to the walls. Now, similar to adiabatic combustion simulation, a simulation can be set up, but with taking the losses from the combustion zone to the walls into account.

The energy balance was based on the measured temperatures to average the enthalpy of the gases at the ports. Even though the temperatures at the ports might not be totally accurate, the inlet and outlet enthalpy levels are specified accurately and hence the overall heat losses will give a realistic picture of the situation. Over the whole furnace the composition was measured on a dry basis and hence the total enthalpies were calculated on a basis of N_2 , O_2 and CO_2 [21].

In Figure 4-6, a general overview with all the energy related processes is shown. Air and fuel are injected with certain energy to the furnace and the fuel is combusted to add additional heat to the inlet enthalpy level. With the temperature and species data from the flue gases, the enthalpy levels at different distances from the burner can be calculated. The differences between the ports can be assumed to be convective and radiative heat losses. The amount of energy lost between two measurement locations is denoted as ΔH in the Figure 4-6 and is the basis of the applied heat losses in the simulations.

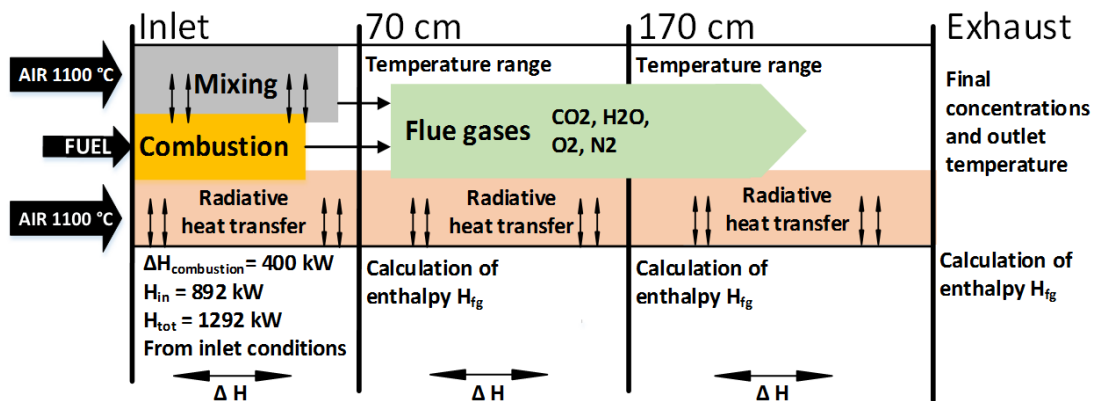


Figure 4-6: Schematic view of the furnace with the inlet streams and the main phenomena having an effect on the energy level inside.

D) Fitting of the temperature profile to the measurement data

The final temperature profile was derived by fitting the calculated NO_x emissions to the measured. An idealized temperature profile shown in Figure 4-7 was used to cover the temperature situation in the furnace. The peak temperature and its position were changed in a way that the detailed chemical reaction scheme results in the measured NO_x levels.

The fitting will help to interpret the validity of the measurement results and give insight how the experimental setup can be improved for the upcoming campaigns.

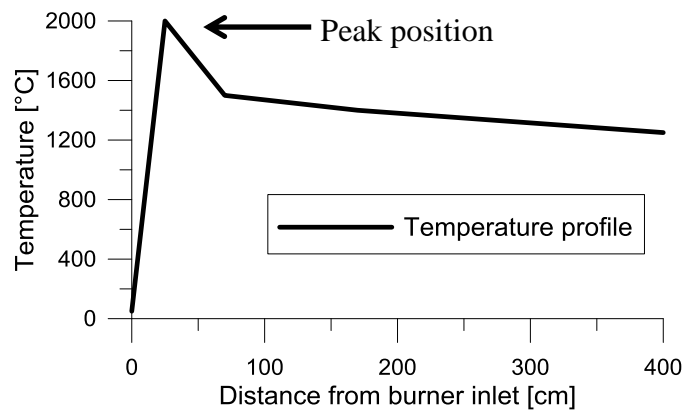


Figure 4-7: Idealized temperature profile shape used for fitting and sensitivity analysis.

Sensitivity analyses of the gas-phase NO_x formation inside the ECF

Having established a model that covers the measured NO_x formation inside the furnace, a sensitivity analysis is carried out on how the NO_x formation varies by changing the parameters shown in Table 4-3. The examined parameters evolved during the previous modelling work, where the results seemed strongly depended on them.

First an analysis of the influence of the peak temperature and the position of the peak is conducted. Their values are changed separately in an idealized temperature profile shown in Figure 4-7.

Table 4-3: Sensitivity analysis parameters of the gas-phase model for NO_x formation.

Parameter	Range
Temperature	1500 – 2300 °C
Peak position	15-30 cm from burner inlet
Mixing	12,5 – 150% of previous mixing

Then for the purpose of indentifying the influence of the mixing behaviour, a new mixing value at 35 cm from the burner inlet is generated. In Figure 4-8 it is shown how this new value is changed from the basic mixing presented in Figure 4-4. With an adiabatic combustion approach it was investigated, which effects the new mixing has on the position of the main combustion.

These new mixing enviroments are applied at two different modelling approaches. The first one involves a fixed temperature at 2100°C and a fixed peak location at 30 cm from the burner location, comparable to Figure 4-7. For the second approach, the information how the position of the combustion changes with the new mixing applied. That means that then the temperature peak position is arranged according to these results, while keeping the peak temperature also at 2050°C.

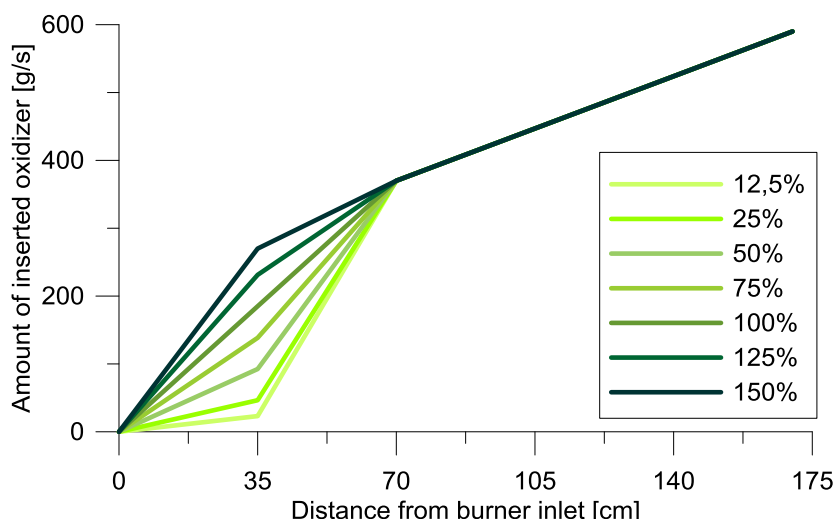


Figure 4-8: Changed mixing behavior for the sensitivity analysis from 12.5 to 150% of the previously used mixing rate at the distance of 35cm from the burner inlet.

Modelling the influence of fuel-NO formation inside the furnace

When calculating the molar nitrogen content of the coals one can find 0.87 mol-% for the coal 1 and around 1.5 mol-% for the Russian Energy coal. With a molar flow of the first coal of 1.5 mol/s and an air flow of 25.4 mol/s and the assumption that all fuel-N is transferred to NO_x , a total of 517 ppm (at 17% excess O_2) of NO_x can theoretically be generated via the fuel-NO route. Having in mind that the Coal 2 has higher nitrogen content than the Coal 1 and the co-firing blends have at least 70% Coal 1 content, it can be said that all the NO_x generated with solid fuel combustion at around 250 ppm can have its origin in fuel-N. Because the solids have a nitrogen component in contrast to liquid and the gaseous fuel experiments, the presence of fuel-bound nitrogen is examined only for them. Therefore in the simulation of the influence of fuel-N, a percentage of HCN is added to the fuel [10].

A) Adding a HCN compound to the fuel

In a first approach, to the model with the temperature and mixing profile from before, a fuel-N compound of 0.87 mol-% (resembling the coal 1) and 1.5 mol-% (resembling the Coal 2) is added. The influence of this fuel-N on the resulting exhaust levels of NO_x is investigated by using the mixing profile from Figure 4-4 and different temperature levels in an idealized temperature profile shown in Figure 4-7.

B) Sensitivity of the conversion of HCN to NO_x

To investigate whether the previous modelling approach of adding HCN to the fuel can cover the fuel-N release sufficiently a sensitivity analysis was carried out with parameters that portray the behavior seen during the solid fuel combustion. In Figure 4-9 new mixing profiles of fuel and oxidizer demonstrate the implementation of delayed burn-up effects and changed mixing behavior.

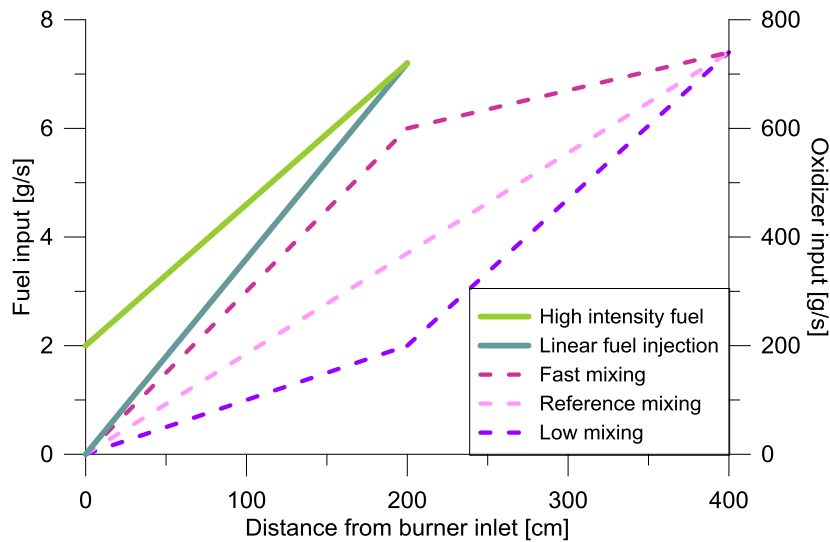


Figure 4-9: Accounting for fuel and oxidizer mixing behavior for solid fuels.

Different solid fuel combustion effects are also implemented by new temperature profiles used in a sensitivity analysis showed in Figure 4-10. There a slightly decreasing slope for co-firing and a more constant slope for coal combustion are plotted. These results are compared against the simplistic approach of only adding a fuel-N component and it is checked, which of the new approaches cover the experimental observations more accurately.

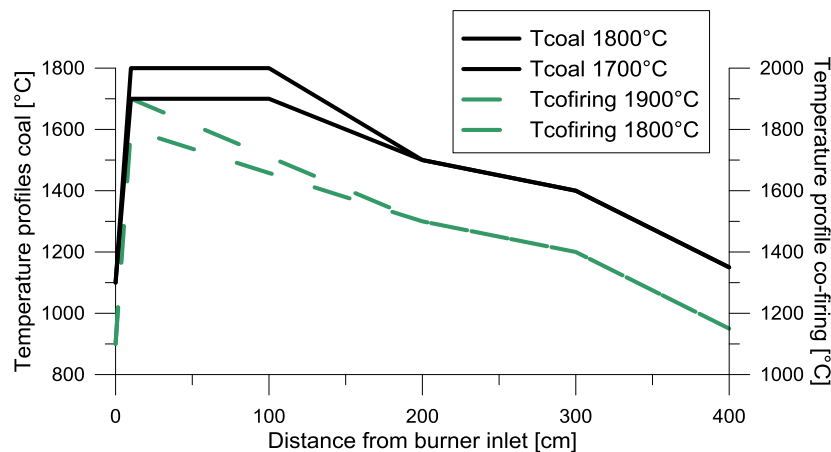


Figure 4-10: Temperature profiles used for the sensitivity analysis of solid fuels.

With the new oxidizer and fuel mixing behavior, different temperature profiles and varying amounts of nitrogen in the fuel, the combustion chemistry was modelled and a sensitivity analysis carried out. Table 4-4 gives a general overview how the parameters were changed. The results are compared to a base case that was set at 0.87 mol-% fuel nitrogen, linear fuel injection and the reference mixing from Figure 4-9 and the temperature profile $T_{\text{coal}} 1800^{\circ}\text{C}$ from Figure 4-10. In the graphs it will also be checked how the modelling results reflect the measurement results of the solid fuel combustion. From this information a possible share of fuel nitrogen contribution to the NO_x exhaust levels inside the ECF will be elaborated and compared to the full scale KK2.

Table 4-4: Sensitivity analysis parameters for the fuel-N release investigation.

Parameter	Range
Fuel-N	0 mol-%, 0.87 mol-%, 1.5 mol-%
Temperature	4 different profiles (peaks at 1700°C – 1900°C)
Mixing	Slower and faster mixing
Fuel injection	Linear injection and more intensive start

Model simplifications

In Table 4-5 the assumptions that were made to simplify the modelling work are described. Most of the assumptions have to be made, because the detailed chemical combustion mechanism does not cover the combustion of long chain hydrocarbons and coal. Furthermore the detailed mixing and flow behaviour inside the kiln are not fully known and also not easily measureable and thus have to be approximated by profiles that comply with the situation between two data points.

Table 4-5: Assumptions to simplify the modelling.

Assumption	Grounds for assumption
Natural gas is modelled as methane.	Natural gas consists mainly of methane and the other short hydrocarbons are considered to decompose fast in shorter chained. The fast decomposition of hydrocarbons is described by Gardiner [11].
Oil is modelled as methane.	Due to high temperatures, an immediate evaporation can be assumed. Gardiner describes the burn up of oil as beginning with a fast decomposition in smaller hydrocarbons and then can be compared to methane combustion [11].
Fuel-N is modelled as HCN.	In a variety of investigations it was found out that fuel-N devolatilizes mainly via NH_3 and HCN [10]. Van der Lans et al. summarize that fuel-N in the conditions of high temperatures and high λ , the dominant released species is HCN.
Coal combustion is examined with a gas-phase modelling approach and methane combustion.	Heterogeneous reactions are difficult to model and are still not fully understood [18]. But according to Warnatz et al. [2], volatiles are mainly CH_4 , H_2 , CO , HCN, which react fast. Furthermore char takes place via oxidation by gas-phase CO_2 and O_2 to CO , which also combusts similar to methane.
Devolatilization effects are modelled as fuel input profile.	Even though the volatiles and char might combust fast, devolatilization takes place over a longer course and thus it will be modelled as a continuous injection of fuel.
Mixing of fuel and oxidizer is represented via a mixing profile of the air.	Difficulties arise explaining kiln aerodynamics precisely, because the exact description of the kiln would require thorough measurements inside the kiln.

5. Modelling NO_x formation

The modelling work described in the following part is used to investigate the levels of NO_x measured and explain differences in combustion phenomena with the help of the detailed combustion mechanism.

5.1. Gas-phase chemistry analysis of experiments

The experimental results showed a similar behaviour of oil and gas during their combustion in the ECF, especially when it comes to the NO_x formation. Coal and biomass showed similar outlet levels, but differed in their speed of combustion. The question raised before was how the NO_x levels of gas and oil can be so much higher compared to the lower emissions for the solid fuels. This is especially a contradicting result, when taking the complete lack of fuel-N into account in natural gas and the very low nitrogen bound in the oil compared to the high amount in coal.

A) Modeled NO_x formation with the measured temperatures as methane combustion

The measured temperature profiles were at first tested in the modelling. The simulations with the all the measured profiles resulted in NO_x outlet concentrations fewer than 10 ppm throughout the fuels.

From these modeling results it can be derived that the measured temperatures were too low for the corresponding NO_x levels, because the simulation and real results deviate by the order of a hundred. It is also possible that other effects, like the fuel-NO formation, that are not covered by the methane combustion model take place for the oil, coal and biomass. But generally it can be derived that the modeling with the measured temperatures does not cover the NO_x formation found in the kiln.

It has to be mentioned that the simplistic mixing profile used was not able to result in the species measured for coal flames, because this profile indicates a lack of oxidizer and hence mixing in the beginning, whereas the experimental results for the coals indicate the constant presence of oxygen. The mixing and the temperatures used could also not resemble the combustion of biomass co-firing flames as they showed measurable carbon monoxide concentrations throughout the reactor, which were not to occur with the rapid methane combustion modelling approach.

B) Adiabatic combustion model of oil and natural gas

As the measured temperature profiles do not give a simple solution of the events leading to the exhaust composition, the NO_x formation needs to be explained in a more detailed way. To begin with analysing the combustion speed, an adiabatic calculation of the combustion situation is carried out. By feeding the mixing behaviour and the inlet conditions of the gases into a simulation, a first impression of both the heating of the fuel and ignition as well as the slope of the temperature profile described in Figure 7-1 is gathered. Adiabatic combustion is assuming that no heat losses occur during the process, what is certainly not the case, but will be covered later.

The temperature peak here is at 2350°C and the position of the peak occurs 22 cm after the burner inlet. Furthermore, the temperature drops sharply afterwards, mostly due to the mixing with more and more combustion air at the temperature of 1100°C.

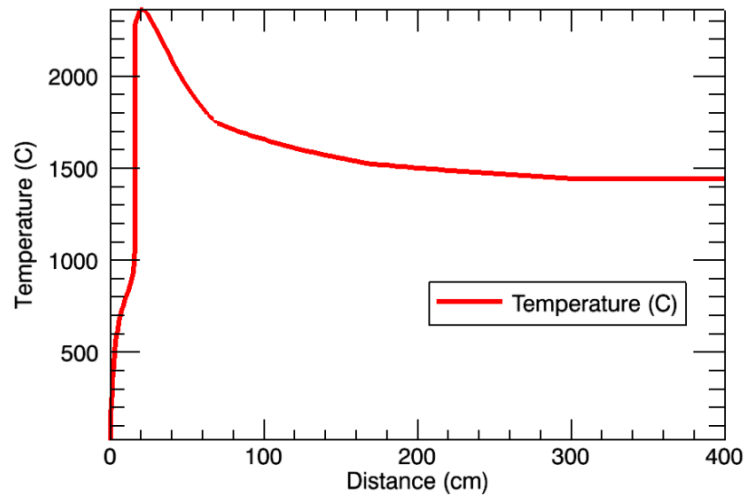


Figure 5-1: Adiabatic flame temperature for the furnace mixing conditions.

Analysis of the reactivity during adiabatic combustion

Related to the model before, the corresponding species during adiabatic combustion are shown in Figure 7-2, where both the CO and the CO₂ concentration climax at 40 cm the latest. This says that the combustion is completed in this distance very short after the burner inlet. The O₂ concentration first rises until the ignition of the fuel starts and all the present oxygen is consumed. The fuel is combusted completely at around 40 cm; the oxygen concentration is converging towards the outlet conditions.

Concluding, the simulation with adiabatic conditions states that there is a very fast combustion of the natural gas close to the burner inlet, which is completed after a very short distance inside the furnace.

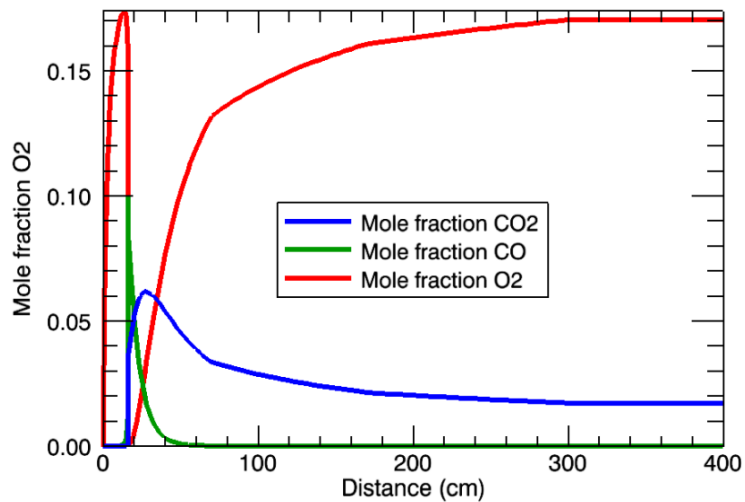


Figure 5-2: Concentrations of CO, CO₂ and O₂ in different burner distances for an adiabatic combustion situation.

C) Heat losses

The heat losses were first calculated via an energy balance over the whole furnace and later also between the different measurement locations inside the ECF. To facilitate the calculations there, the temperatures of 1400°C for port 2 and 1300°C for port 4 were used for calculations with oil and natural gas. These temperatures were well within the temperatures measured in this main combustion zone.

The balance over the whole furnace accounted for heat losses of 0.30 kJ/cm s. The more complex results for the calculations of the different ports are shown in Tables 7-1 and 7-2. One can see that also this point of view shows high similarity of oil and gas combustion and so only the oil calculation was used.

Table 5-1: Heat losses from the furnace for oil combustion.

Heat loss	Amount [kW]	Distance [cm]	Heat loss per unit length [kW/cm]
$\Delta H_{in,port\ 2}$	91.1	70	1.38
$\Delta H_{port2,port4}$	93.6	170	0.93
$\Delta H_{port4,out}$	185.0	~1200	0.18

Table 5-2: Heat losses from the furnace for natural gas combustion.

Heat loss	Amount [kW]	Distance [cm]	Heat loss per unit length [kW/cm]
$\Delta H_{in,port\ 2}$	96.6	70	1.4
$\Delta H_{port2,port4}$	93.1	170	0.9
$\Delta H_{port4,out}$	184.0	~1200	0.18

Both the constant and the varying heat losses were fed into the modelling to convert the adiabatic combustion into non-adiabatic with heat losses and see what effects that has on the slope of the temperature.

Two different shapes of the heat loss distribution were applied in Figure 7-3. A constant heat loss in the left Figure and the heat losses, which are linked to the temperature data from the measurements, in the right Figure. The constant heat loss did not change the peak temperature significantly compared to the calculations without any heat losses. Hence, one can say that the first approach may not cover the radiative heat losses from the flame to the wall at the burner inlet. This is the reason for a very high peak temperature, before the flame is cooled down to the same levels as in the second case. On the contrary, the high heat loss from the beginning in the second plot may give rise to the assumption that the ignition is delayed too much. The temperature peak drops thereby to 1950°C.

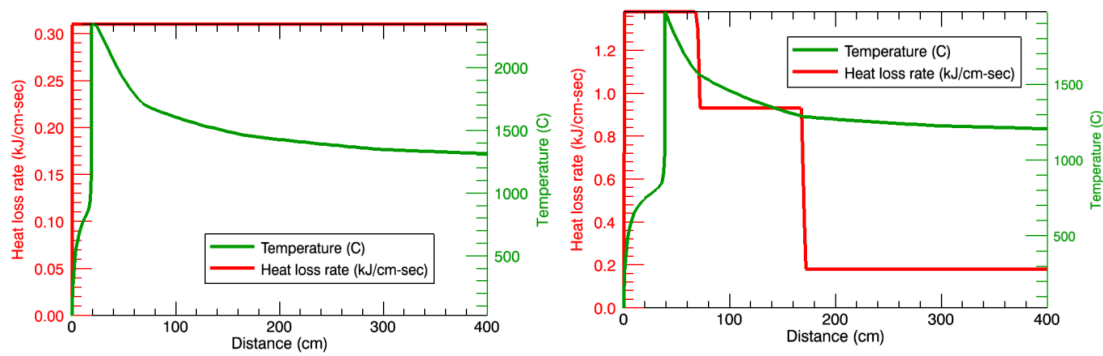


Figure 5-3: Temperature profiles with different heat loss distributions, A) constant heat losses between inlet and outlet, B) heat losses linked to the temperature measurements.

NO_x formation during combustion

The two temperature profiles found with the heat losses were then examined for their resulting NO_x levels and compared to the measurement data from the natural gas and oil fuels shown in Figure 7-5. The plotted experimental data was averaged over the main combustion zone to equal the modelling approach with the mixing profile. The distance at 400 cm describes the outlet conditions.

The lower model meaning a low temperature peak leads to low NO_x formation and an exhaust of 260 ppm. The higher model with the 2350°C peak seems to capture the formation pattern quite accurate, but a lot too high. The temperature reaches there the same peak as in the adiabatic model. The main NO_x formation takes place before the 70 cm measurement point and presumably in the temperature peak, whose position was found during the adiabatic analysis. The low NO_x formation for the flame of 1950°C gives rise to the assumption that the actual temperature in the flame was higher than this value, but lower than 2350°C.

D) Fitting the model to the experimental data

With the information from the adiabatic calculations, a simplified temperature profile inside the furnace was developed and fitted to results of the measured NO_x levels in port 2 and 4. Different positions of the peak and peak temperatures can cause the found NO_x concentration.

Figure 7-4 shows the results of possible peak temperatures in relation of the peak location to reach the measured NO_x levels. The plot says that for the creation of 1200 ppm at port 2, 800 ppm at port 4 and an outlet of around 650 ppm, these temperatures have to prevail in front of a certain distance of the burner. The NO_x formation of the fitted temperature profile is shown with the other modelling results in Figure 7-5.

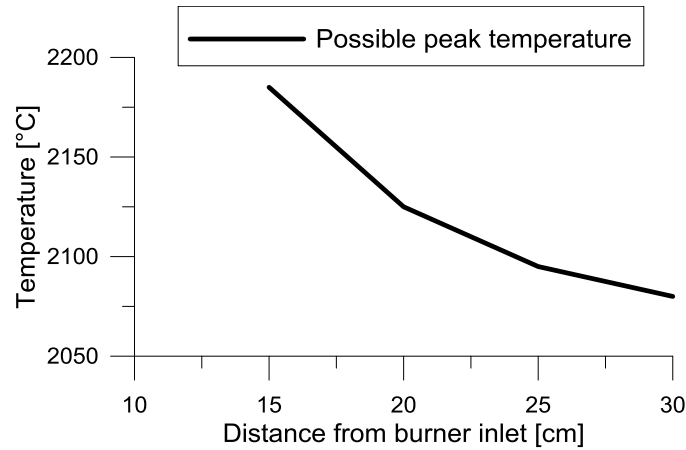


Figure 5-4: Results of fitting the peak temperature and peak location to the measured NO_x levels.

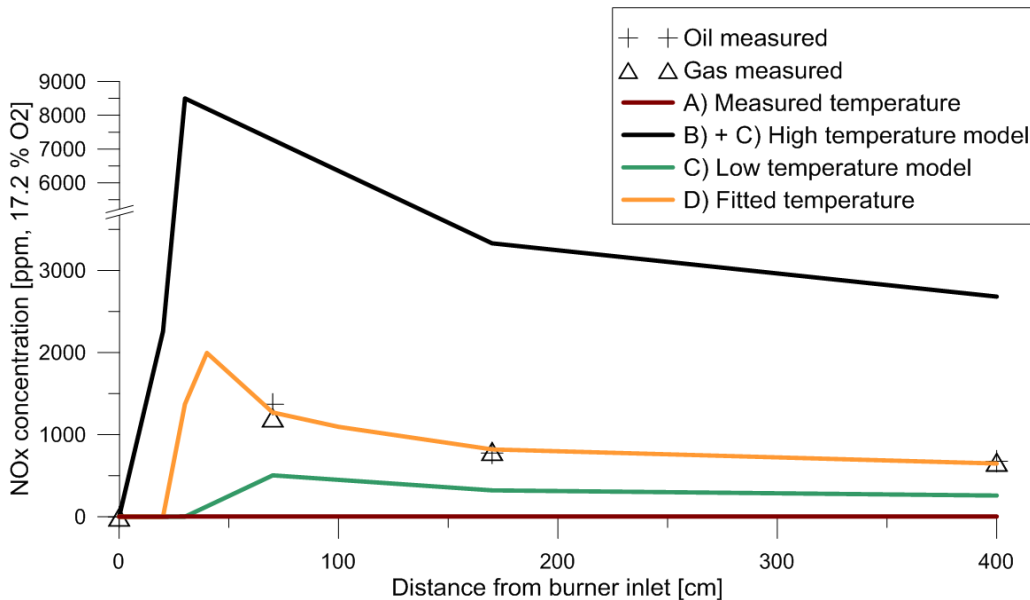


Figure 5-5: Comparison of NO_x generation of the simulation results with the measurements. A)-D) indicate the different temperature profiles used in the modelling from the section above.

NO_x chemistry in the ECF

Figure 7-6 presents NO_x chemistry inside the furnace with the fitted temperature profile described above with a peak temperature of 2095°C , 25 cm away from the burner inlet. At the onset of the combustion at around 5-10 cm from the burner inlet, the hydrocarbon radicals present are consumed extremely fast. The formation of NO_x through that route has, thus, a neglectable impact on total NO_x formation. Simulations with lower temperature peaks gave NO_x formation of 5 ppm for 1600°C which can be seen as the part of formed prompt-NO during the combustion.

The thermal-NO formation peaks shortly after the temperature and is the major source of NO_x . The short delay of the formation peak relative to the temperature peak could be explained by that in the high temperature region first radicals are generated that react further to NO_x . In this region also the amount of oxygen is low, because not enough oxidizer has mixed into the combustion zone yet. In the Figure 7-6 no NO_x is

formed after 50 cm anymore. The temperature is around 1800°C at this distance and the of activity of the thermal-NO mechanism declines.

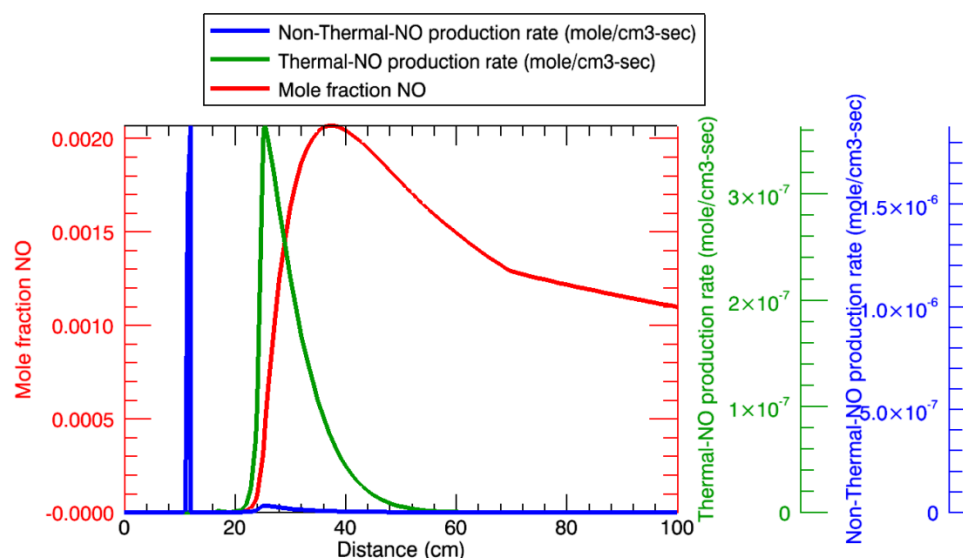


Figure 5-6: Thermal and Non-Thermal-NO formation rates for 2095°C peak at 25 cm. (The scale of the distance was reduced).

5.2. Summary of the gas-phase chemistry modelling

The modeling results show clearly that the measured temperatures do not comply with the measured concentrations. Simulations with the experimental temperatures produced much lower NO_x concentrations than measured. With temperatures profiles estimated from the overall heat balance, the combustion experiments with oil and gas were well represented by the simulations with methane. As expected the combustion of biomass has a different combustion process than the one seen with methane.

Observations of adiabatic combustion and the combustion chemistry showed a very fast combustion of oil and gas within the first 15 cm - 40 cm after the burner inlet, where no measurements were taken. The modeling results show temperature levels over 2050°C that are necessary to produce the measured NO_x exhaust. Thermal formation of NO_x totally dominates the NO_x formation for the combustion of oil and gas.

During the course of the modeling work it was found out that the temperature, the mixing pattern and temperature peak location have a major impact on the formation of nitrogen oxides and are therefore subject of a sensitivity analysis.

5.3. Sensitivity analysis for gas-phase chemistry

Sensitivity of the NO_x formation for different temperature peaks

The peak temperatures and the peak location are diametrically important to NO_x outlet concentrations. In accordance with the modeling results before, the peak is most probably occurring in some distance after 20 cm from the burner inlet. The next modeling analysis is therefore dedicated to the effects of the temperature levels for 4 different peak locations of 20 cm, 25 cm, 30 cm and 35 cm.

In Figure 7-7, the results for the temperature sensitivity are plotted for the 4 different peak locations. It is shown that the peak location has some effect for the exhaust NO_x concentration, especially the hotter the peak temperature gets in the range above 2000°C. But what can be seen more clearly is the decisive influence of the temperature on the NO_x formation. Considerable amounts of NO_x can only be generated if the combustion gases stay above temperatures of 1900°C for a sufficient long time. The formation itself accelerates exponentially above this temperature.

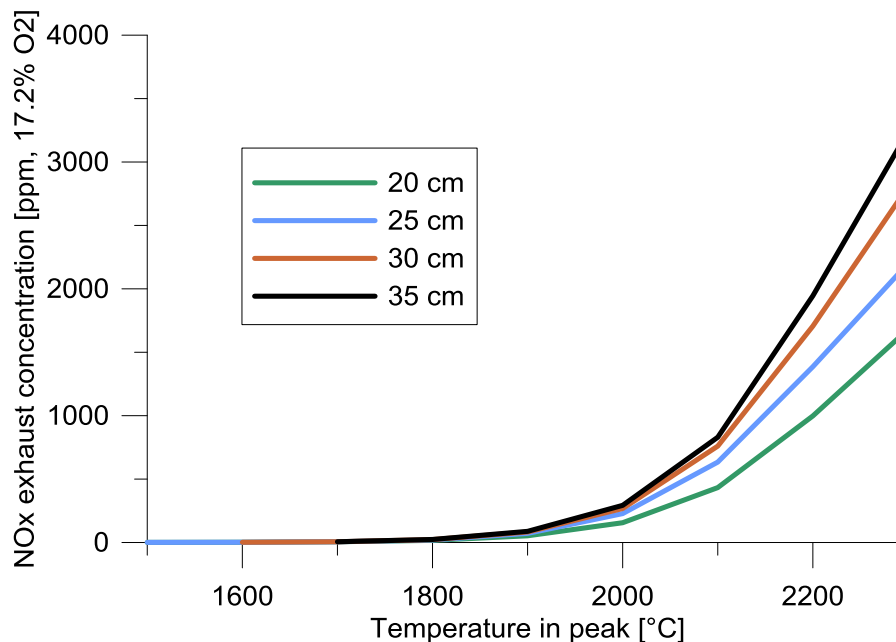


Figure 5-7: NO_x exhaust concentration for different temperature peak locations in relation to the temperature in the peak.

Sensitivity of the NO_x formation related to the mixing behavior

A sensitivity analysis of the mixing behaviour between the inlet and the first measurement positions (70 cm) is carried out. This region turned out to be crucial to the NO_x formation inside the furnace. With the new mixing behaviour at 35 cm distance of the burner new adiabatic calculations of the furnace were conducted. The adiabatic calculations did not change the peak temperatures, thus, the NO_x formation was basically the same for all new mixing behaviours at 2350°C. In all the adiabatic cases around 2600-2800 ppm of NO_x were formed. Just the position of the temperature peak and with it the thermal-NO peak changed from 13 cm after the burner inlet for 150% mixing of air to 43 cm for 12.5% mixing.

The approach with the adiabatic temperatures did not result in any hints of how a different mixing pattern is influencing the NO_x outlet conditions, but it showed that

the main combustion zone will move closer or away from the burner inlet. To examine this effect, two cases were tested. The first one involves a fixed temperature profile with a peak of 2100°C and only the mixing is changed. The second test case has also a peak temperature of 2100°C but the position of the peak is arranged from the results of the adiabatic calculations. For faster mixing (150% of reference) the combustion moves to 13 cm from the inlet. For slower mixing the peak moves to 43 cm.

The results of the two approaches are shown in Figure 7-8. Assuming a fixed peak and a fixed temperature, a different mixing could provide enormous potential to mitigate NO_x according to the simulation results. In the fixed temperature case, the potential shows up to be 90% lower NO_x levels when reducing the mixing by 87.5%. The later case included the effects of lower mixing on the temperature peak. This is assumed to resemble the reality more likely, but then also shows lesser NO_x reduction, maxing at around 50%.

The result of the fixed peak location shows that the amount of oxidizer and with it the present oxygen in the peak is a key factor for thermal-NO generation. The lesser amount of oxygen present at this point, the lesser the NO_x formation. In reality it can be assumed that a worse mixing will also slow the reaction and therefore the peak will occur later, where again more oxygen is present. So for the more realistic varied peak, the NO_x mitigation potential is lower. For the modelling itself it means that the exact mixing information is not that important for the stability of the results, as long as the peak position is arranged to fit chemical reactions inside the furnace.

For the sake of completeness it has to mentioned that the temperature was kept at 2100°C for the different mixing behaviours. A worse mixing will possibly also lead to a lower peak temperature, so that the mitigation effect could be bigger than the results shown here.

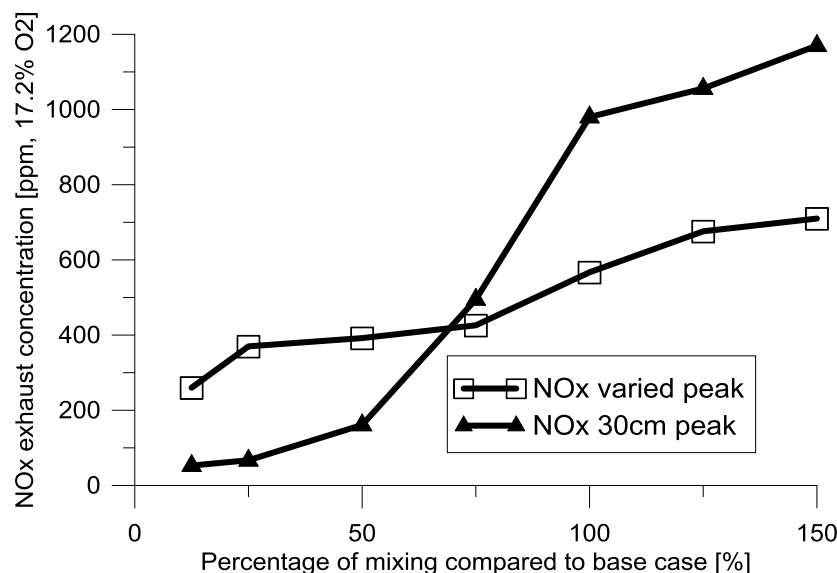


Figure 5-8: NO_x generated considering different mixing patterns at 2100°C peak temperature. For the first graph, the peak position was varied according to the adiabatic calculation results. The second graph shows the influence of mixing with a fixed temperature peak.

5.4. Impact of fuel nitrogen on NO_x formation

During the combustion of coal and the biomass co-firing it was discovered that the combustion is not restricted by the mixing rate of oxidizer and fuel, but more the combustion of the particles itself was the limiting process for the reaction velocity. The steady built up of NO_x could not be explained with the methane combustion model.

Sensitivity analysis of the impact of fuel nitrogen

In Table 7-3 the differences in the simulations by adding 0.87 mol-% and 1.5 mol-% of HCN as a devolatilization source of Fuel-N to the methane combustion model are presented. Generally, the difference is around 30 ppm. It seems that for higher temperatures, larger amounts of HCN follow the route towards NO. From the simulations of both 0.87 mol-% and 1.5 mol-% it is found out there is not a certain percentage of HCN converted to NO_x, because the NO_x yields only slightly differ.

Table 5-3: Effects of adding fuel-N in the form of HCN compared to a case without Fuel-N. Methane combustion and temperature peak at 25 cm from the burner inlet. NO_x measured at 17.2% O₂. In this table, the NO_x levels of the pilot and full scale units fired with and without fuel-N are indicated as ECF and KK2 respectively.

	HCN 0 mol-%	HCN 0.87mol-%	HCN 1.5 mol-%
Temperature	NO _x [ppm]	NO _x [ppm]	NO _x [ppm]
1500°C	3	31	37
1600°C	4	32	36
1700°C	10	37	42
1800°C	29	59	64
1900°C	93 KK2_{oil}	125 KK2_{coal}	130
2000°C	273	315 ECF_{coal} + ECF_{bio}	323
2100°C	740 ECF_{oil} + ECF_{gas}	784	790
2200°C	1544	1610	1623

In these simulations with fuel-N, still the major part of the NO_x that is formed in the ECF has to be generated via the thermal-NO route, because only 30-65 ppm of the 280 ppm for coal 1 could be connected to the fuel-N contribution. The conversion rate of fuel-N to NO_x ranges from 5.8% at 1500°C to 13.5% at 2100°C.

At the full scale KK2, it can be assumed that around 70 ppm of nitrogen oxides are linked to the conversion of fuel-N to NO_x, from the difference of oil and coal combustion there. Assuming that the combustion of oil causes slightly higher peak temperatures than coal there, even 90-100 ppm of NO_x via the fuel-NO route are probable for the coal. In Table 7-3 it is shown that higher temperatures promote the formation of NO_x from fuel bound nitrogen. Taking this into account, it seems more realistic that more than 100 ppm of the 280 ppm in the ECF stems from the fuel-NO route.

Reaction path analysis of Fuel-N

The comparison of the fuel-N modelling results with the full scale unit was contradicting, so that the chemical analysis of the modelling with HCN was examined in more depth in Figure 7-9. There one can see that the HCN is consumed fast while moving towards the peak location and is fully converted before 20 cm. Thereby only around 7% of the HCN is converted to NO_x . Conversion rates for fuel bound nitrogen to NO_x are usually found above 20%. [9] This together with the comparison with the full scale indicates that modelling with HCN from the beginning will convert bigger parts of it towards N_2 than can be expected in reality.

The chemical modelling of the solid particle combustion as a methane flame deviates also too much from the measurements of the species CO and CO_2 inside the furnace. From the measurements, the fuel-N can be assumed to be released over a longer period of time, during the particle burn-up and not entirely from the beginning as shown in Figure 7-9. Furthermore, with the whole fuel modelled as inserted from the beginning, the combustion will lead to a period of time, where no oxygen is present, what was not measured for the coal and only for a small part of the co-firing experiments.

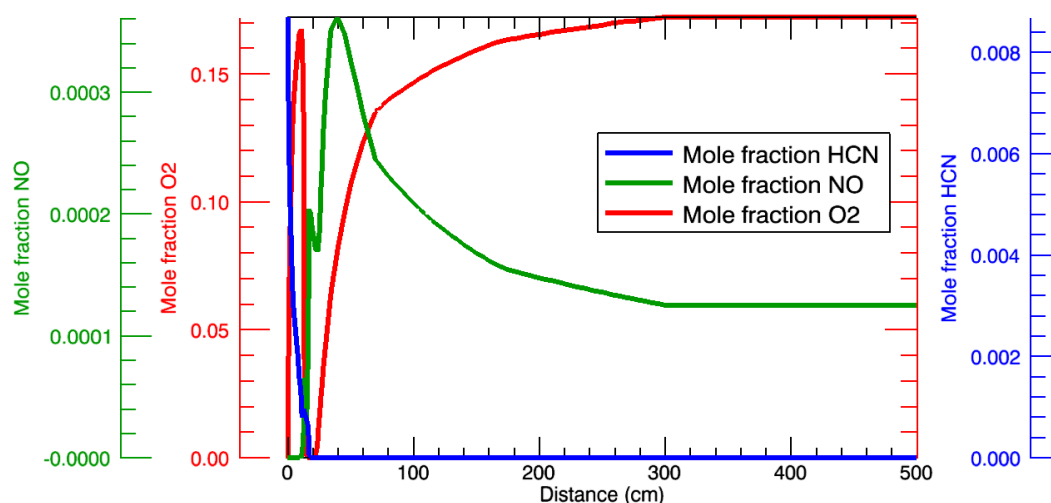


Figure 5-9: Modelled species for solid particle combustion as a methane flame with 0.87mol-% HCN added. Simplified mixing and temperature profiles as shown before with 1900°C peak temperature at 25 cm distance from the burner.

Gas-phase modelling approach to cover fuel-N release

From the chemical analysis it becomes quite clear that the approach used sophisticatedly for oil and gas shows some serious drawbacks for the coal and co-firing combustion. For the solid fuels a new modelling environment has to be created to cover the effects seen during the experiments, which were:

- NO_x was measured already at 20 cm distance for both burners, what supposed the early presence of oxygen in the combustion zone. When all fuel is modelled from the beginning, an oxygen lean situation would be created that was not present in reality
- CO was measured throughout all ports, which indicates an ongoing fuel burn-up, whereas the methane modelling proposing instantaneous burn-up.

- Constant NO_x built-up for the coal burner indicates high temperatures over a longer period than before and/or the ongoing release of Fuel-N.
- Built-up of CO_2 throughout the furnace.

The described phenomena showed to be not able to model with the assumption that all fuel is inserted at the beginning, because this would lead to complete absence of oxygen in the first part of the furnace. In this oxygen lean situation, the formation of NO_x is strongly limited, what contradicts the measurement results.

With new mixing profiles and a continuous fuel injection, the measured O_2 and CO_2 concentration from the experiments are fairly well represented by the model. Figures 7-10 and 7-11 show the chemical species of the modelling with the changed modelling environment. The first case for the coal is now able to represent the effect of continuous combustion and a NO_x formation that is increasing towards port 2. CO_2 is formed throughout the furnace, but because of the big amounts of air mixed into the combustion zone, the levels are constant.

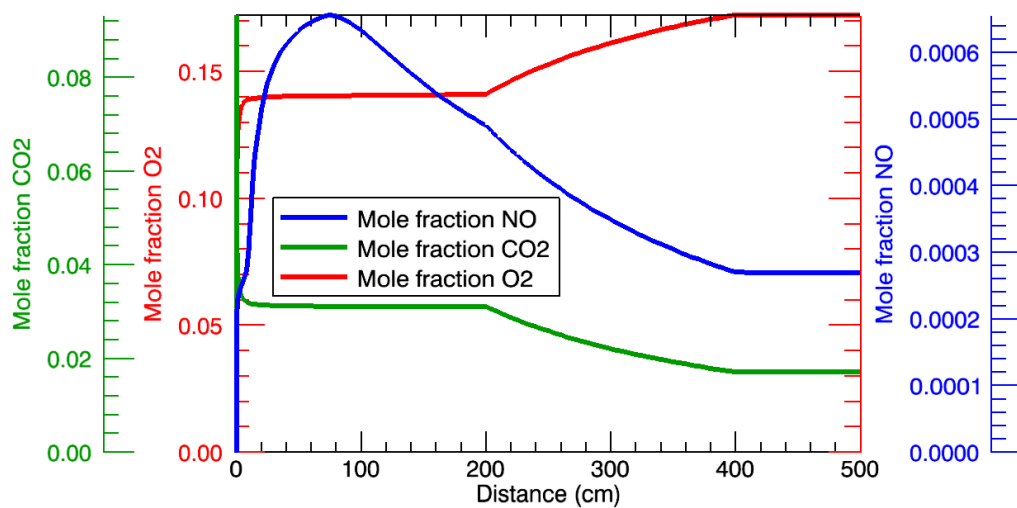


Figure 5-10: Modelling result for a coal temperature profile at 1700°C, continuous fuel injection and a simplified oxidizer mixing. 0.87 mol% HCN as Fuel-N added.

The co-firing experiment in Figure 7-11 was modelled with a fuel injection that is more intensive in the beginning, but continuous over a long distance in the reactor. With this the very high CO_2 levels in the beginning can be reproduced, but also the early NO_x built-up effect is gained. Both approaches lead to a conversion rate of fuel-N to nitrogen oxides of over 20% or a contribution of more than 100 ppm. This is due to the fact that this time not all the HCN is reacting in a high temperature and oxygen lean environment, which is found close to the burner inlet in the approach before.

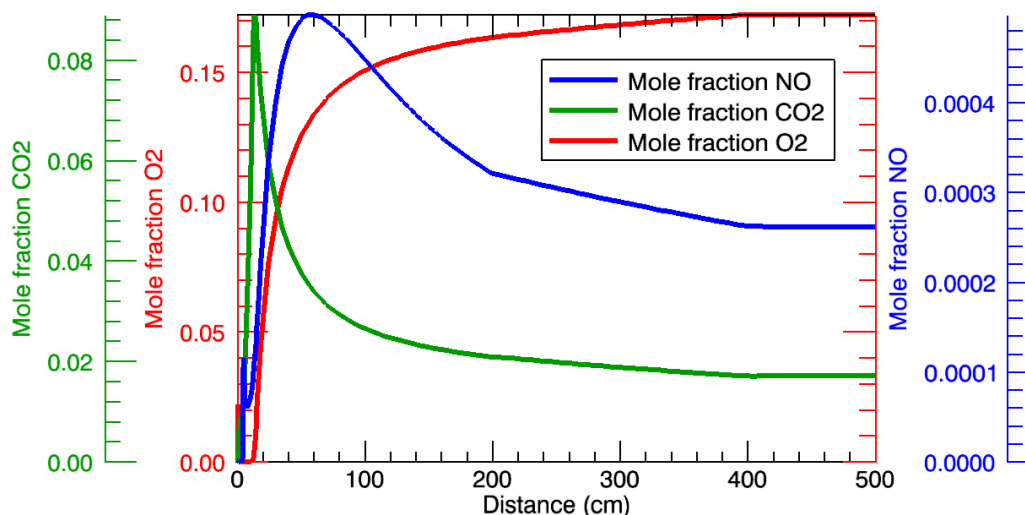


Figure 5-11: Modelling result for a co-firing temperature profile at 1800°C, continuous fuel injection with stronger injection in the beginning and a simplified oxidizer mixing. 0.87 mol% HCN as Fuel-N added.

5.5. Sensitivity analysis of the fuel-NO contribution

Proving that the new modelling approaches cover the chemistry inside the kiln more accurately, a sensitivity analysis is carried out to see the influence of each single parameter on the model. Within the sensitivity analysis, added Fuel-N, different temperature levels, different fuel injection and oxidizer mixing patterns are varied, to see which modelling results finally compare to the measurement results.

Fuel-N contribution to NO_x formation

In Figure 7-12, a linear fuel injection into the furnace was used to cover the effect of an ongoing release of volatiles and burn-up of fuel. For the used temperature profile, the NO_x originating from the 0.87 mol-% HCN, which was used to model the fuel-N compound, was then around 130 ppm. For 1.5 mol-%, around 230 ppm of fuel-NO was formed more compared to the case without any fuel-N contribution. This corresponds to a fuel-N conversion rate for both HCN concentrations of 27%. In this modelling approach, the fuel-NO_x accounts for around 50% of the total NO_x created.

Modelling the fuel-N without the influence of the thermal-NO route (below 1500°C) gave an outlet concentration of 140 ppm. This shows that the fuel-N contribution is quite independent of the temperature situation at the general conditions inside the ECF. Comparing the simplistic approach with all the fuel modelled from the beginning and the ramped injection of the fuel, the position inside the furnace and the combustion conditions there determine which amount of fuel-N is later forming NO_x or N₂.

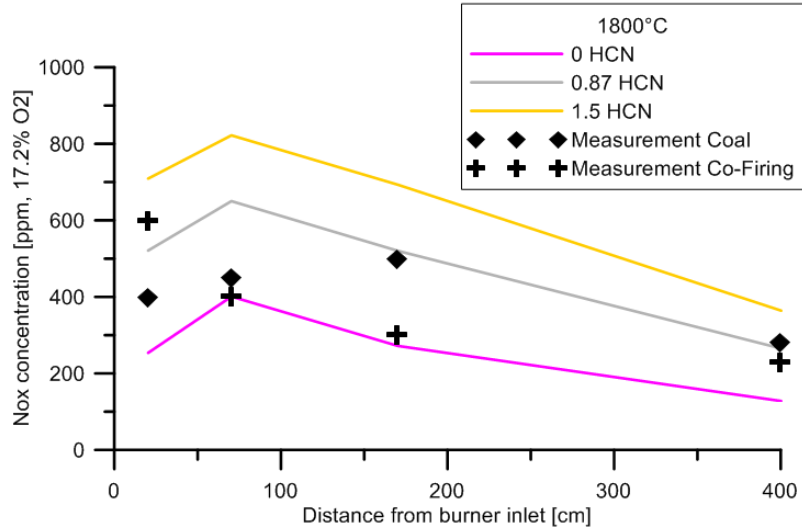


Figure 5-12: Influence of fuel-N on total NO_x formation. Fuel-N modelled as HCN compound in fuel.

Thermal NO influence on total NO_x levels

In the gas-phase modelling the thermal-NO_x formation was rising exponentially with the temperature, when crossing the border of around 1800°C. The same conclusion can be drawn from the modelling of the solid fuels. The rise of 100°C in temperature will double the NO_x formation as can be seen in Figure 7-13. The thermal-NO formation is still the key criteria for lower overall NO_x emissions.

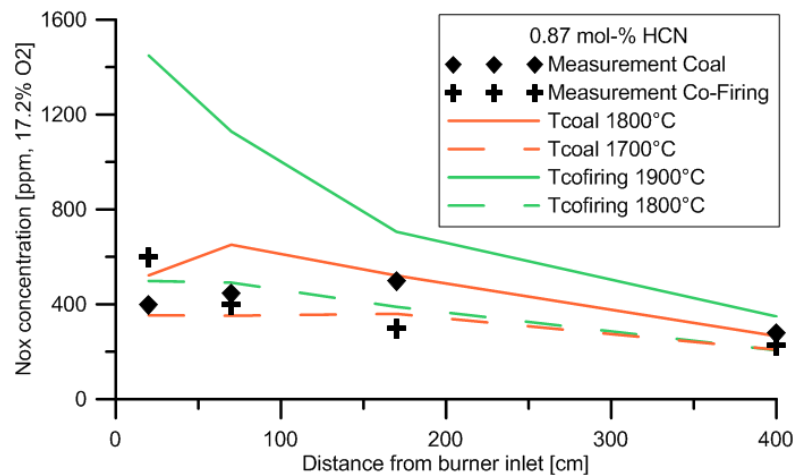


Figure 5-13: Influence of different temperature levels on total NO_x formation.

The influence of the fuel injection pattern to the furnace

It was described that the combustion during the co-firing was more intense close to the burner than the combustion with the reference burner. To examine this effect, the fuel release was modelled with two different fuel release behaviors. In Figure 7-14 it can be proven that an early release of the fuel will lower the overall NO_x emissions. This has already been seen before, when the complete fuel was inserted in the beginning of the modelling.

The high amount of fuel is reducing the oxygen present during the time when HCN is converted and therefore the route towards N_2 instead of NO_x is more promoted, the earlier the fuel is released in the furnace.

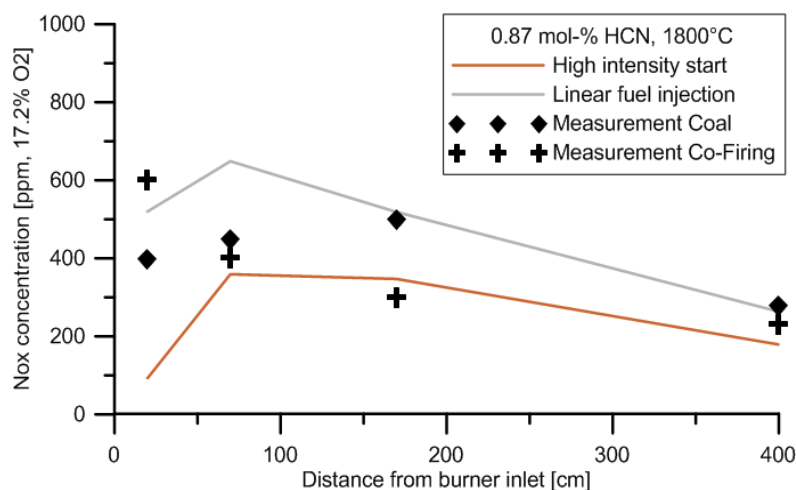


Figure 5-14: Influence of difference fuel release profiles on the total NO_x formation.

Influence of the mixing behavior

Varying the speed in which the oxygen is mixed into the main combustion zone showed no big influence on the total NO_x levels during the combustion at 1800°C, unlike detected for the gas-phase modelling at 2050°C. In Figure 7-15 it seems more like a certain amount of NO_x is generated that is just diluted at different speeds by differing the mixing behaviors. It has to be noted that still all the mixing patterns account for continuous oxygen rich conditions, because the fuel is inserted gradually. For the modelling this means that the amount of NO_x formed is quite independent from the mixing behavior and so the size of the modelled combustion zone is arranged by the mixing pattern.

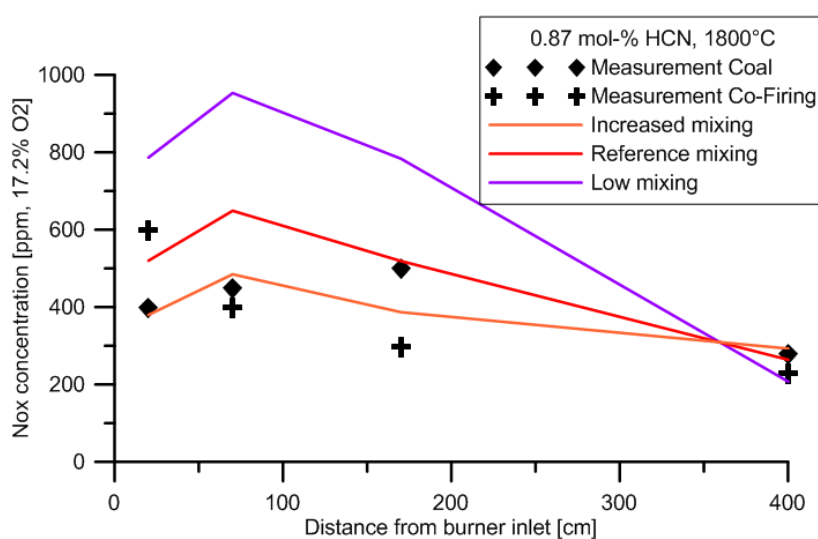


Figure 5-15: Influence of the oxidizer mixing on the total NO_x formation.

5.6. Summary of the modelling work on fuel nitrogen

Adding a usual fuel-N devolatilization component, HCN, to the methane increased the NO_x formation by around 30 ppm. The HCN to N₂ conversion was in this case surprisingly fast and at a distance of 20 cm more than 90% of the HCN was converted to N₂ and less than 10% HCN was later found as NO_x.

A gradual injection of fuel into the main combustion zone, simulating the release of volatile nitrogen gave more reasonable results with respect to in-furnace NO_x, O₂ and CO₂ concentrations. Because solid fuels can be described better with a continuous combustion than with an instantaneous one like gas and oil, this injection pattern was used thereafter.

With the new injection pattern of fuel, it was found out that the timing of the release of the HCN compound is of high significance for lowering NO_x emissions. An early release will promote the conversion of HCN to N₂. The reason for this occurrence could be both the lower concentration of oxygen and the higher temperatures during the early time in the reactor.

The mixing of oxygen has in this approach only a minor influence on the NO_x exhaust, because almost throughout the furnace there is an abundance of oxygen. But as before, the temperature is the key factor in avoiding NO_x emissions. The detailed chemical reaction mechanism also indicates a promotion of the conversion of fuel-N to NO_x at higher temperatures.

In summary, the modelling results show that between 10%, for fast combustion, to 30%, for the ramped combustion, of the fuel bound nitrogen is later found as NO_x. This corresponds to 50 – 150 ppm of fuel-NO_x contribution. In the ECF a total of around 250 ppm was found, so the corresponding share is 20% - 60%. In the KK2, 100-125 ppm total NO_x emissions are found. Hence, the fuel bound nitrogen can contribute to 50-100% of the total NO_x emissions there. Assuming that especially the first modelling approach with the whole HCN modelled from the beginning underestimates the importance of fuel-N, the fuel NO_x contribution is considered to be higher for both plants than 20% and 50% respectively.

In Table 8-1, the results for the furnaces are summarized. The results show clearly that the combustion situation is different in the ECF compared to the KK2 unit. The combustion is several hundred degrees hotter in the pilot scale ECF leading to other NO_x formation behavior than in the full scale kiln.

Table 5-4: Comparison of the different furnaces according to their NO_x formation.

Parameter	ECF coal/BM	ECF gas/oil	KK2 coal	KK2 oil
Peak temperature	1700 – 1850 °C	2050 – 2180°C	<1700°C	~ 1850°C
Total NO _x	~250 ppm	~680 ppm	100 – 125 ppm	50 – 115 ppm
Fuel-NO _x of total NO _x	30-60%	0%	70-100%	0%

6. Conclusions

In this work, the formation of nitrogen oxides in a rotary kiln test facility was examined. For this purpose, the data of an experimental campaign was evaluated and the nitrogen chemistry inside the furnace modelled.

The experimental evaluation revealed problems with the position of the main combustion zone and the measured temperatures. In Table 8-1 it is shown that coal and biomass led generally to lower NO_x formation than oil and gas inside the ECF. The full scale plant KK2 instead exhausts considerably lower emissions for both oil and coal, but in contrast to the ECF, the oil causes even lower NO_x formation there than coal.

Because the real temperatures in the kiln remained not totally clear after the measurement campaign, the contribution of thermal-NO to the total concentration can only be examined accurately for oil and gas, because there it is by far the major contributor. The gas-phase modelling for these two fuels revealed that peak temperatures of over 2000°C had to be present inside the experimental furnace to cause the measured NO_x levels, but only around 1500°C were measured.

The sensitivity analysis of the gas-phase chemistry showed that the NO_x formation in the kiln is highly dependent on the temperature in the furnace. Mixing of fuel and oxidizer as well as the position of the temperature peak, have minor influence on the formation.

For solid fuel combustion the quantity of NO_x formation that can be traced to fuel-N was investigated. In a sensitivity analysis it was shown that the fuel- NO_x accounts for roughly the half of the NO_x emissions and considerable amounts are formed via the thermal- NO_x route in the ECF. This is in contrast with the full scale KK2 plant, where NO_x from the fuel bound nitrogen prevails. The conversion of fuel-N to NO_x is strongly dependent on the time, when the nitrogen is released.

7. Proposals for future campaigns

The main aim of this work was to elaborate proposals to improve the oncoming measurement campaigns and their research outcome.

7.1. Improving the measurement quality

The main problems seen within the campaign were the temperature measurements, which were found to be too low to meet the other measurements data and the position of the flame. So the first thing to improve is the arrangement of the temperature probe, especially its gas inlet velocity, so that it can measure sufficiently in this high temperature environment. With correct temperature measurements, more accurate estimates of the thermal-NO formation can be conducted.

The shifted position of the flame poses also a possible source of error for the correct modelling of the NO_x formation. The oil, gas and coal reference burner have to be investigated if they are creating the shifted flame. A possible examination could consist of mounting the burners in different angles compared to the former installation to investigate if the burners create the defect. It can also be possible that the air inlets create the flame shift and therefore the investigation of a reduced or increased flow through the air hoods could shed light if this effect creates the fluctuations.

The missing measurements for oil and gas combustion at port 1 are a major drawback not only for the modelling of the two fuels but also to draw conclusions for the overall gas-phase modelling of the ECF. It was shown that the combustion is very fast inside the ECF close to the burner. Hence the measurements at port 2 could only capture the outcome of the combustion. But for the later examination of heterogeneous reaction paths, the detailed knowledge about the gas-phase reactions at this point is indispensable.

7.2. Comparing NO_x formation in full scale and pilot scale

The KK2 unit produces exhaust levels of around 110 ppm during the combustion of coal and to some extent lower emissions for oil. In the ECF the effect was opposite, because oil and gas released 2.5 times higher emission of NO_x than coal. Generally, the ECF produced distinctly higher levels for all fuels ranging from 215 ppm to 680 ppm. The measurement campaigns during the ULNOX project pointed at a limited comparability of the two furnaces and also this work comes to the conclusion that the combustion situation inside both differs sharply.

The difference between coal and oil in the KK2 is described by the contribution of fuel-N from the coal. NO_x formed during the combustion of oil can mainly be linked to thermal-NO formation. The somewhat higher peak temperatures occurring for oil are overcompensated by the fuel-NO.

In the ECF instead, the main contribution is triggered by the high temperatures that must beat the temperatures in the KK2 by at least 100°C to generate the measured NO_x exhaust levels. A more precise specification of the difference fails not only by the lack of correct measurement data of the ECF, but also a detailed examination of the flame and combustion situation inside the KK2 is missing.

To get information from experiments at the ECF that can be applied also at full scale, the shape of the flame and its peak temperature is a key factor. The flow situation is shown to be of minor importance. Therefore extensive temperature measurements are

necessary inside the full scale kiln. But also correct temperature measurements inside the ECF could facilitate the examination of different fuels with their fuel-N release and speed of combustion.

7.3. Future modelling of the NO_x formation

As soon as the temperature measurements are accurate they can be included as input factors into the modelling work and then give precise information of the thermal-NO formation. A modelling approach should investigate how far the gas-phase chemistry is independent of the presence of fuel-N in the furnace. With information of the interaction of thermal and fuel generated NO_x, first precise evaluation of thermal-NO for solid fuels can be derived and afterwards the fuel-NO contribution estimated accurately. Also a more detailed analysis of the heterogeneous NO_x formation mechanisms can be carried out to check how the particles interact with the gases.

Knowing where and how much fuel-NO is formed will help to develop models that can predict the outcome of several mitigation strategies. The major drawback so far is the lack of knowledge of how the fuel-N path is influenced by the high amount of oxidizer present and the very high temperatures.

When thinking about the KK2 it could be beneficial to have a simplistic gas-phase model of the chemical reactions inside it as well, to have a reference to compare the results. Therefore the oil combustion could be examined and directly compared to the same situation in the ECF. This information could then help, to make the ECF more comparable to the full scale unit.

8. Bibliography

- [1] World Steel Association , "WORLD STEEL IN FIGURES 2013," World Steel Association, Brussels, 2013.
- [2] J. Warnatz, U. Maas and R. W. Dibble, Combustion - Physical and Chemical Fundamentals, Modeling and Simulation, Experiments, Pollutant Formation, 2nd ed., Berlin: Springer Verlag, 1996.
- [3] K. Meyer, Pelletizing of Iron Ores, Berlin: Springer-Verlag, 1980.
- [4] LKAB, "Operation Areas," 11 01 2012. [Online]. Available: <http://www.lkab.com/en/About-us/Overview/Operations-Areas/>. [Accessed 24 04 2014].
- [5] C. A. Tuck and R. L. Virta, "2011 Minerals Yearbook," U.S. Department of the Interior/ U.S. Geological Survey, Reston, 2013.
- [6] C. Fredriksson, "COMBUSTION IN ROTARY KILNS AT LKAB," in *IFRF Finnish-Swedish Flame Days*, Jyväskylä, 2013.
- [7] L. Nils-Olov and P. Kostamo, "BAT examples from the Nordic iron and steel industry," Nordic Council of Ministers, Copenhagen, 2006.
- [8] R. Remus, M. A. Aguado Monsonet, S. Roudier and L. Delgado Sancho, "Best Available Techniques (BAT) Reference Document for Iron and Steel Production," Publications Office of the European Union, Luxembourg, 2013.
- [9] P. Glarborg, A. Jensen and J. Johnsson, "Fuel nitrogen conversion in solid fuel fired systems," *Progress in Energy and Combustion science*, pp. 89-113, 2003.
- [10] R. Van Der Lans, P. Glarborg and K. Dam-Johansen, "Influence of process parameters on nitrogen oxide formation in pulverized coal burners," *Progress in Energy and Combustion Science*, pp. 349-377, 1997.
- [11] W. Gardiner Jr., Gas-Phase Combustion Chemistry, New York: Springer Science+Business Media, 2000.
- [12] J. Zeldovich, "The Oxidation of Nitrogen in Combustion and Explosions," *Acta Physicochimica*, pp. 577-628, 1946.
- [13] C. Fenimore, "Formation of nitric oxide in premixed hydrocarbon flames," *Symposium (International) on Combustion*, pp. 373-380, 1971.
- [14] T. Mendiara and P. Glarborg, "Ammonia chemistry in oxy-fuel combustion of methane,"

Combustion and Flame, pp. 1937-1949, 2009.

- [15] J. A. Miller, M. C. Branch and R. J. Kee, "A Chemical Kinetic Model for the Selective Reduction of Ammonia," *COMBUSTION AND FLAME*, pp. 81-98, 1981.
- [16] Ø. Skreiberg, P. Kilpinen and P. Glarborg, "Ammonia Chemistry below 1400 K under fuel-rich conditions in a flow reactor," *Combustion and Flame*, pp. 501-518, 2004.
- [17] P. Dagaut, P. Glarborg and M. Alzueta, "The oxidation of hydrogen cyanide and related chemistry," *Progress in Energy and Combustion Science*, pp. 1-46, 2008.
- [18] F. Normann, Oxy-Fuel Combustion - The control of Nitrogen Oxides (PhD - Thesis), Göteborg: Reproservice, Chalmers University of Technology, 2010.
- [19] H. Thumann, S. Andersson, P.-E. Bengtsson, B. Leckner, G. Palchonok and D. Pallares, "Combustion Engineering," Reproservice, Chalmers University of Technology, Göteborg, 2014.
- [20] M. V. Heitor and A. Moreira, "Thermocouples and Sample Probes for Combustion Studies," *Progress in Energy and Combustion Science*, pp. 259-278, 1993.
- [21] S.-E. Mörstedt and G. Hellsten, DATA OCH DIAGRAM, Stockholm: Liber AB, 2008.
- [22] A. Ponzio, S. Senthooresvan, W. Yang, W. Blasiak and O. Eriksson, "Ignition of single coal particles in high-temperature oxidizers with various oxygen concentrations," *Fuel*, pp. 974-987, 2008.
- [23] A. Ponzio, S. Senthooresvan, W. Yang, W. Blasiak and O. Eriksson, "Nitrogen release during thermochemical conversion of single coal pellets in highly preheated mixtures of oxygen and nitrogen," *Fuel*, pp. 1127-1134, 2009.